RNA-seq and scRNA-seq reveal trajectory progression of the retinal ganglion cell lineage in wild-type and *Atoh7*-null retinas

Fuguo Wu[1,2,*], Jonathan E. Bard[2,*], Julien Kann[2], Donald Yergeau[2], Darshan Sapkota[1,2], Yichen Ge[1,2], Zihua Hu[2], Jie Wang[3], Tao Liu[3], Xiuqian Mu[1,2]

[1]Department of Ophthalmology/Ross Eye Institute, University at Buffalo, Buffalo, NY
[2]New York State Center of Excellence in Bioinformatics and Life Sciences, University at Buffalo, Buffalo, NY
[3]Department of Biostatistics & Bioinformatics, Roswell Park Comprehensive Cancer Center, Buffalo, NY

Short title: Developmental trajectory of the retinal ganglion cell lineage

Corresponding author: Xiuqian Mu, 701 Ellicott Street, Buffalo, NY, 14203. Tel: 001-716-881-7463; Fax: 001-716-849-6651; Email: xmu@buffalo.edu

* These authors contributed equally to this project.

Key Words: Retinal development; Neural development; Transcription factors; Retinal ganglion cells; Gene regulation; bHLH transcription factors; Single cell RNA-seq

Abstract:

Formation of retinal ganglion cells (RGCs) is governed by a hierarchical gene regulatory network with key transcription factors such as Atoh7, Pou4f2 and Isl1 functioning at different levels. Past studies concluded that Atoh7 is critical for the emergence of the RGC lineage in the developing retina, whereas Pou4f2 and Isl1 function further downstream. Atoh7 is expressed in a subset of retinal progenitor cells (RPCs) and is considered a competence factor for the RGC fate, but the molecular properties of these RPCs have not been well characterized. In this study, we first used conventional RNA-seq to investigate transcriptomic changes in *Atoh7*-, *Pou4f2*-, and *Isl1*-null retinas at embryonic (E) day 14.5 and identified the differentially expressed genes (DEGs), which expanded our understanding of the scope of downstream events regulated by these factors. We then performed single cell RNA-seq (scRNA-seq) on E13.5 wild-type and *Atoh7*-null retinal cells using the 10X Chromium platform. Clustering analysis not only correctly identified known cell types at this developmental stage, including RPCs, RGCs, cones, and amacrine/horizontal cells, but also revealed a transitional cell state which was marked by *Atoh7* and genes for other lineages in a highly overlapping fashion and shared by all early developmental trajectories. These results provide significant insights into the nature of RPC competence for different retinal cell fates and the likely mechanism by which these fates are committed. Further, analysis of the *Atoh7*-null retina not only identified the affected genes/pathways involved in the different cell states but also revealed that in the absence of Atoh7, the RGC lineage still progressed considerably and a substantial amount of RGC-specific gene expression still occurred. Thus, Atoh7 likely collaborates with other factors to shepherd the transitional RPCs to the RGC lineage by competing with other lineage factors and activating RGC-specific genes. This study thus revises our current view on the emergence of the RGC lineage and shed new light on the general mechanisms governing retinal cell differentiation.

Introduction

The central nervous system has the most diverse cellular composition in the animal body. How this complexity is achieved during development has been one of the central questions of neuroscience. In the central nervous system, all neural cell types originate from a common pool of neural progenitor cells; neural progenitor cells take on different developmental trajectories to eventually assume distinct cell fates. The neural retina is an ideal model for studying neural development. All retinal cell types arise from a single population of retinal progenitor cells (RPCs) through a conserved temporal sequence, but with significant overlaps (Cepko, 2014; Cepko et al., 1996; Livesey and Cepko, 2001; Young, 1985). The competence of RPCs for different cell fates change over the course of development so that different cell types are produced at different time windows (Austin et al., 1995; Belecky-Adams et al., 1996; Cayouette et al., 2003; Gomes et al., 2011; La Vail et al., 1991; Rapaport et al., 2004; Reh and Kljavin, 1989; Wong and Rapaport, 2009; Young, 1985). Several factors influencing the temporal change of RPC competence have been identified (Clark et al., 2019; Gordon et al., 2013; La Torre et al., 2013; Mattar et al., 2015). However, multiple retinal cell types are often born in overlapping time windows, but the nature of RPC competence for individual cell types remains unknown. Based on gene expression, considerable heterogeneity has been observed within the general RPC population, which may be related to their competence for the various retinal cell fates (Brzezinski et al., 2011; Fu et al., 2009; Hafler et al., 2012; Kiyama et al., 2011; Li et al., 2004; Mu et al., 2005a; Nishida et al., 2003; Trimarchi et al., 2008). In agreement with this idea, many key regulators, mostly transcription factors, expressed in subsets of RPCs have been shown to regulate different steps of retinal cell fate specification and differentiation (Brown et al., 2001; Emerson et al., 2013; Fujitani et al., 2006; Li et al., 2004, 2004; Nakhai et al., 2007; Nishida et al., 2003; Sapkota et al., 2014; Wang et al., 2001). Several RPC subpopulations including those expressing *Atoh7*, *Olig2*, *Neurog2*, and *Ascl1* have been shown to be essential or biased for certain fates (Brzezinski et al., 2011, 2012; Feng et al., 2010; Hafler et al., 2012). However, the cell states in which these key transcription factors operate in, the actual complexity of RPC heterogeneity, the relationships between the different RPC sub-populations, and their relevance to RPC competence for individual retinal fates, have only begun to be addressed. Conventional experimental approaches have provided much insight into the genetic pathways and mechanisms underlying the formation of various retinal cell types (Bassett and Wallace, 2012; Cepko, 2014; Swaroop et al., 2010; Xiang, 2013). However, the traditional approach of investigating individual genes and cell types has been painstakingly slow-paced and inefficient in providing a comprehensive picture, since genesis of many cell types often occurs in overlapping time and space. Understanding the relationships among different progenitor subtypes and the progression of individual cell lineages is often limited by the knowledge of marker genes, the availability of proper reagents, and the low throughput and resolution and low qualitative nature of conventional multiplexing assays. Recent development in transcriptomics analysis using next-generation sequencing, particularly at single cell levels, affords powerful means to survey the complexity of cell composition and progression of cell states for individual cell lineages.

Single cell expression profiling (single cell RNA-seq, scRNA-seq) uses microfluidic devices to isolate single cells and generate barcoded cDNA libraries. The libraries are then sequenced by next-generation sequencing (Macosko et al., 2015; Zheng et al., 2017). The sequence reads can then be decoded and attributed back to specific genes in individual cells, and expression levels of individual genes within each cell can then be determined. This approach enables the expression profiles of thousands of individual cells to be analyzed, and the cells can then be grouped (clustered) based on their similarities. The groups of cells thus identified from a developing tissue can reveal cellular complexity of the tissue and the different cell states of individual cell lineages during development. The technology has been adopted to study many developing tissues and organs including the retina (Clark et al., 2019; Giudice et al., 2019; Lukowski et al., 2019; Macosko et al., 2015; Menon et al., 2019; Rheaume et al., 2018; Shekhar et al., 2016; Sridhar et al., 2020; Tran et al., 2019), and can thus be used to analyze the heterogeneity of RPCs and their relationships to different retinal lineages. The current study focuses on one of the early retinal cell types, retinal ganglion cells (RGCs). Three key transcription factors, Atoh7, Pou4f2, and Isl1, function at different stages along the RGC lineage. Atoh7 functions prior to the RGC fate is determined and is essential, but not sufficient, for the RGC fate (Brown et al., 2001; Brzezinski et al., 2012; Feng et al., 2010; Mu et al., 2005a; Wang et al., 2001; Yang et al., 2003), whereas Pou4f2 and Isl1 function to specify the RGC fate and promote RGC differentiation (Erkman et al., 1996; Gan et al., 1996; Mu et al., 2008; Pan et al., 2008; Wang et al., 2000). Atoh7 has thus been considered a competence factor. However, how the RGC lineage emerges in the global context of retinal development and what specific roles Atoh7 plays in this process is not well understood.

To further understand RGC differentiation, we first performed conventional RNA-seq on mutant E14.5 retinas of the three key transcription factors genes, *Atoh7*, *Pou4f2*, and *Isl1*, to characterize the global downstream events during RGC development. This allowed us to expand the scope of downstream genes from previous studies and obtain a global view on the functions of these key regulators. We then performed scRNA-seq on retinal cells from E13.5 wild-type and *Atoh7*-null retinas. At this stage, only four early retinal cell types, RGCs, horizontal cells, amacrine cells, and cones, are being generated (Young, 1985). Our analysis not only identified all these retinal cell types with unique gene signatures but also revealed their relationship to the RPC groups. Importantly, we discovered that all the early cell lineages went through a shared transitional cell state before the cell fates were committed, and that this state was marked by such genes as *Atoh7* and *Otx2* that are involved in the formation of these lineages. Analysis of the *Atoh7*-null cells revealed that the RGC trajectory was truncated as expected, with major changes in gene expression in individual cell types/states, particularly in RGCs. Unexpectedly, the RGC lineage still formed and advanced substantially, indicating that other factors are involved in establishing this lineage. These results provide novel insights into the cellular and genetic mechanisms governing the emergence of the different retinal lineages and advance our understanding of the cellular process and genetic pathways underlying the establishment of the RGC lineage.

Material and methods

Animals

All mice used were in the C57BL6/129 mixed genetic background. The *Atoh7*-null mice used was a knock-in line in which a zsGreen-T2A-CREERT2 cassette replaced the *Atoh7* coding region. This allele manifests the same defects in RGC development as previously reported with other *Atoh7* knockout alleles (Brown et al., 2001; Wang et al., 2001; Wu et al., 2015) and will be published separately. All procedures using mice conform to the U.S. Public Health Service Policy on Humane Care and Use of Laboratory Animals and were approved by the Institutional Animal Care and Use Committees of Roswell Comprehensive Cancer Center and University at Buffalo.

Conventional RNA-seq

Conventional RNA-seq was carried out as previously described (Sapkota et al., 2014). After timed mating, E14.5 retinas were dissected and stored in RNAlater (Invitrogen) while genotyping was performed. Three individual pools of four to six retinas were collected for individual genotypes, including wild-type, *Atoh7*-null, *Pou4f2*-null, and *Isl1*-null. Total RNA was then isolated and RNA-seq libraries were generated using TruSeq RNA Sample Prep Kit v2 kit (Illumina, RS-122-2001) following the manufacturer′s instruction and sequenced on an Illumina HiSeq2500 sequencer. Sequence reads were mapped to the mouse genome assembly (mm10) by STAR (Dobin et al., 2013) (https://github.com/alexdobin/STAR) and differentially expressed genes (DEGs) were identified by EdgeR (Robinson et al., 2010) (https://bioconductor.org/packages/release/bioc/html/edgeR.html). The FDR cutoff was set at 0.05 and the minimum fold change imposed was 1.5. To compare gene expression changes in the three mutants, we calculated the z-score of sequence read counts per million (CPM) for each gene, then divided the genes into five groups based on the hierarchical clustering. We then generated a heatmap of differential genes by the "pheatmap" R package (https://cran.r-project.org/web/packages/pheatmap/index.html). All RNA-seq sequence reads were deposited into the NCBI Short Read Archive (accession numbers SAMN02614558-SAMN02614569).

Retinal cell dissociation, scRNA-seq library construction, and library sequencing

Dissociation of embryonic retinas into single cell suspensions was performed as previously described (Wu et al., 2012). E13.5 retinas with the desired genotypes were collected after timed mating. They were then washed with cold phosphate buffered solution, pH7.0 (PBS), and transferred to fresh tubes containing 200 µl 10 mg/ml trypsin in PBS. The retinas were then incubated in a 37˚C water bath for 5 mins and triturated five times with a P1000 pipette tip. 20 µl of soybean trypsin inhibitor was then added to the tube. The cells were spun down at 500 g, washed twice with PBS, and resuspended in PBS. The cells were then loaded onto the 10X Genomics Chromium Controller to generate scRNA-seq libraries using the Chromium Single Cell 3' Library & Gel Bead Kit v2, following the manufacturer's instructions. The libraries were sequenced by an Illumina

HiSeq2500 rapid run using 26x8x98 sequencing. were deposited into the NCBI Short Read Archive with accession numbers from XXXX to XXXX.

scRNA-Seq Analysis

The output from 10X Genomics Cellranger 2.1.1 pipeline was used as input into the R analysis package Seurat version 3.1.1. Cells with high unique molecular index counts (nUMI), high mitochondrial transcript load, and high transcript counts for red blood cell markers were filtered out from the analysis. The data was then r normalized, scaled, and explored using Seurat's recommended workflow. Principal component analysis (PCA), louvain clustering, and the UMAP (Uniform Manifold Approximation and Projection) were performed. Using the called clusters, cluster-to-cluster differential expression testing using the Wilcoxon Rank Sum identified unique gene markers for each cluster. Differential expression between shared wild-type and mutant clusters was assessed using the FindMarkers function of Seurat, which also utilized the Wilcoxon Rank Sum test. Cell cycle analysis used a protocol in Seurat with 70 cycle genes (Tirosh et al., 2016) (https://satijalab.org/seurat/v3.1/cell_cycle_vignette.html).

To further interrogate the RGC developmental trajectory, cells belonging to C3, C4, C5 and C6 were subset from the Seurat data object. The average expression for each DEG, for each cluster, was compared between wildtype and *Atoh7*-null mice using the pheatmap package, clustering rows by euclidean distance using the hclust algorithm, and introducing cuts to the hierarchy tree using cutree = 7 for visual clarity.

Pseudotime Analysis

In order to infer developmental trajectories, the python package SCANPY provides pseudotemporal-ordering and the reconstruction of branching trajectories via Diffusion Pseudotime (DPT) (Haghverdi et al., 2016). A root cell was selected at random within the progenitor cell population of called Cluster 1. The assigned pseudotime values was then mapped back to the Seurat UMAP embedding for visualization and further analysis.

In situ hybridization and online data mining

In situ hybridization was performed using RNAscope double Z probes (Advanced Cell Dignostics) on paraffin-embedded retinal sections. After timed mating, embryos of desired stages were collected, fixed with 4% paraformaldehyde, embedded in paraffin, sectioned at 6 µm, and de-waxed, as previously described (Mu et al., 2004, 2008; Sapkota et al., 2014; Wu et al., 2015). The sections were then processed, hybridization was performed, and the signals were visualized using the RNAscope® 2.5 HD Detection Reagents-RED following the manufacturer's manual. Images were collected using a Nikon 80i Fluorescence Microscope equipped with a digital camera and Image Pro analysis software.

Results

Changes in gene expression in *Atoh7*-, *Pou4f2*-, and *Isl1*-null retinas

Atoh7, Pou4f2, and Isl1 are three key regulators in the gene regulation network controlling RGC development (Mu et al., 2008; Wu et al., 2015). They function at two different stages; Atoh7 is believed to confer competence to RPCs for the RGC lineage, whereas Pou4f2 and Isl1 function to specify the RGC fate and promote differentiation. Previously, downstream genes of Atoh7, Pou4f2, and Isl1 have been identified by microarrays (Mu et al., 2004, 2008; Qiu et al., 2008). However, due to limitations of the technology used, those genes likely only cover small proportions of those regulated by the three transcription factors. To gain a more global view of the function of the three transcription factors, we collected total RNA samples from wild-type, *Atoh7*-null, *Pou4f2*-null and *Isl1*-null retinal tissues at E14.5 and performed RNA-seq. The RNA-seq data from the wild-type retina provided a comprehensive list of genes expressed in the E14.5 retina with at least 1.0 average counts per million reads (CPM, see Suppl. Table 1). We then identified differentially expressed genes (DEGs) by edgeR (Robinson et al., 2010) in each of these mutant retinas as compared to the wild-type retina using a cutoff of at least 1.5 fold change and FDR of at least 0.05 (Suppl. Tables 2-4). In the *Atoh7*-null retina, we identified 670 downregulated genes, and 293 upregulated genes (Suppl. Table 2); in the *Pou4f2*-mull retina, we identified 258 downregulated genes and 169 upregulated genes (Suppl. Table 3); and in the *Isl1*-null retina, we identified 129 downregulated genes and 79 upregulated genes (Suppl. Table 4). These genes not only confirmed previous findings, as essentially all previously identified DEGs were included, but also provided a more complete picture by significantly increasing the numbers of DEGs for each mutant. The different number of DEGs in these three mutant retinas was consistent with their severity of defects in RGC development (Brown et al., 2001; Gan et al., 1999; Mu et al., 2008; Pan et al., 2008; Wang et al., 2001), which was further reflected by a clustering heatmap analysis, showing that the *Atoh7*-null retina was least similar, and the Isl1-null retina was most similar, to the wild-type retina (Figure 1A)

Consistent with RGCs being largely missing in the *Atoh7*-null retina, RGC-specific genes were mostly found in the downregulated DEG list, whereas RPC-expressed DEGs included both down- and upregulated genes (Suppl. Table 2). The downregulated Atoh7 gene list also encompassed the majority of genes in downregulated Pou4f2 and Isl1 lists, as would be expected considering that Pou4f2 and Isl1 function downstream of Atoh7 (Figure 1B). Gene ontology (GO) analysis by DAVID (Huang et al., 2009) found the genes in all three downregulated genes lists were highly associated with different aspects of neural differentiation, as demonstrated by enriched biological processes and GO terms (data not shown). The smaller number of genes affected in the *Pou4f2*- and *Isl1*-null retinas reflected the fact that Pou4f2 and Isl1 are downstream of Atoh7, and that they only represent a part of the downstream events along the trajectory of RGC development. On the other hand, the three upregulated gene lists were markedly different and much less overlapped (Figure 1C, Suppl. Table 2-4). This likely reflected that these three factors repress gene expression largely independently at two different levels of the gene regulatory hierarchy either directly or indirectly; Atoh7 represses gene expression in proliferating RPCs, confirming our previous analysis (Mu et al., 2005a), whereas *Pou4f2* and *Isl1* repress gene expression in RGCs. Independent gene repression by these factors

was also demonstrated by genes with changes in different directions in these three mutant retinas (Suppl. Table 2-4). For example, *Nhlh1* did not change in *Atoh7*-null, was down-regulated in *Pou4f2*-null (fold change -2.2), but upregulated in *Isl1*-null (fold change 1.7), whereas its related gene *Nhlh2* was down-regulated (fold change -2.0) in *Atoh7*-null, did not change in *Pou4f2*-null, but was significantly up-regulated in *Isl1*-null (fold change 1.7). We also confirmed that some marker genes for amacrine cells (e.g. *Chat*, *Th,* fold change 383.0 and 35.1 respectively) were markedly up-regulated in *Pou4f2*-null as previously reported (Qiu et al., 2008), but they did not change in either *Atoh7*-null or *Isl1*-null retinas. *Dlx1* and *Dlx2*, two genes involved in RGC development (de Melo et al., 2005; Zhang et al., 2017), were down-regulated in the *Atoh7*-null retina, but up-regulated in the *Pou4f2*- and *Isl1*-null retinas, indicating these genes were activated by Atoh7 in RPCs, but repressed by Pou4f2 and Isl1 in RGCs (Suppl. Table 2-4).

The DEG lists also revealed/confirmed that key pathways were affected in the three mutant retinas and additional components were found to be affected. For example, the Shh pathway, which is under the control of the gene regulatory network for RGC genesis, plays a key role in balancing proliferation and differentiation through a feedback mechanism (Mu et al., 2004, 2005b, 2008; Pan et al., 2008; Wang et al., 2005). Expanding previous findings, we found more components in the Shh pathway were affected in all three mutant retinas (Figure 2A). These component genes, including *Shh*, *Gli1*, *Ptch1*, *Ptch2*, and *Hhip*, revealed a complex feedback loop of the pathway in balancing proliferation and differentiation via downstream genes such as *Gli1* and *CcnD1* (Cyclin D1) (Figure 2B). Consistent with this model, *Gli1* and *CcnD1* expression was reduced in all three mutants (Suppl. Table 2-4). Multiple component genes of the Notch pathway, including *Hes2*, *Hes5*, *Dll1*, *Jag1*, were upregulated in the *Atoh7*-null, but not the other two mutant retinas. This further supported that Atoh7, but not Pou4f2 or Isl1, repress gene expression in RPCs, since the Notch pathway plays key roles in RPC proliferation (Suppl. Tables 2-4) These results further demonstrated that deletion of *Atoh7* not only compromised RGC formation but also altered the properties of RPCs.

Single cell RNA-seq of wild-type and *Atoh7*-null retinas

Whereas the RNA-seq data provided much insight into gene regulation by Atoh7, Pou4f2, and Isl1 in the developing retina, how their absence affected different cell states could not be attained. Particularly for Atoh7, it functions in a subset of RPCs that give rise to RGCs, but the properties of these RPCs and their relationships to other cell populations have not been well characterized. To that end, we performed single cell RNA-seq with E13.5 wild-type and *Atoh7*-null retinal cells. The choice of E13.5, instead of E14.5, was fortuitous but did not affect our overall analysis since largely the same cell types are being generated in these two time points (Cepko et al., 1996; Young, 1985). After filtering out blood cells, doublet cells, and stressed cells, we were able to obtain expression data of 3521 wild-type cells and 6534 *Atoh7*-null cells. The median sequence reads were 68,491 and 54,765 for wild-type and mutant cells respectively. The median numbers of genes captured were 1,975 and 2,375 for wild-type and mutant cells respectively. UMAP

clustering was then performed on these cells using Seurat 3.1.1 (Stuart et al., 2019), which resulted in a total of 11 clusters (C0-C10) for both wild-type and *Atoh7*-null cells, and the corresponding clusters highly overlapped (Figure 3A, B). We first used known marker genes to assign identities to these clusters. These markers included *Ccnd1* and *Fgf15* for naïve RPCs (Mu et al., 2005b; Trimarchi et al., 2008), *Atoh7* and *Otx2* for subpopulations of RPCs (Brown et al., 1998; Fu et al., 2009; Nishida et al., 2003), *Pou4f2* and *Pou6f2* for RGCs (Xiang et al., 1995; Zhou et al., 1996), *Ptf1a* and *Tfap2b* for amacrine and horizontal precursor cells (Fujitani et al., 2006; Nakhai et al., 2007), *NeuroD4* and *Crx* for photoreceptors (Akagi et al., 2004; Furukawa et al., 1997; Mu et al., 2005a), and *Otx1* and *Gja1* for ciliary margin cells (Calera et al., 2006; Zhao et al., 2002). At this stage, horizontal cells and amacrine cells seemed not to have fully diverged yet and thus were grouped together (Figure 3A, B). These marker genes were specifically expressed in distinct clusters as demonstrated by dot plots (Figure 3C, only data for wild-type cells are shown) and feature plot heatmaps (Suppl. Figure 1). This allowed us to definitively designate their identities, including three clusters as naïve RPCs (C0-C2), two as transitional RPCs (C3 and C4) for reasons further discussed below, two as RGCs (C5 and C6), one as horizontal and amacrine precursors (C7), two as photoreceptors (cones) (C8 and C9), and one as ciliary margin cells (C10). Notably and as expected, *Atoh7* was absent and the two RGC markers *Pou4f2* and *Pou6f2* were markedly diminished in the *Atoh7*-null cells (Suppl. Figure 1), but the corresponding clusters in which they were expressed in the wild-type, including the two transitional RPC clusters (C3, C4) and two RGC clusters (C5, C6), still existed. Marker genes for the other mutant clusters did not show overt changes in their expression (Suppl. Figure 1). These results were consistent with previous knowledge that RGCs, horizontal cells, amacrine cells, and cones are the major cell types being generated at this developmental stage (Cepko et al., 1996; Young, 1985), and that deletion of *Atoh7* specifically affects RGCs (Brown et al., 2001; Wang et al., 2001).

We also performed cell cycle analysis following a protocol in Seurat 3 using 70 cell cycle markers (Tirosh et al., 2016) and found that, for both wild-type and *Atoh7*-null cells, the three naïve progenitor cell clusters C0-C2 roughly co-segregated with their positions in the cell cycle, C0 in G1 and early S, C1 in S and G2/M, and C2 in G2/M. The transitional RPCs (C3, C4) were also actively proliferating as they were found in different phases of the cell cycle, C3 in S and G2/M and C4 in G2/M (Figure 3D, E). On the other hand, clusters composed of differentiating cells (C5, C6, C7, C8, C9) were all in G1/0 phase, confirming that they were indeed postmitotic neurons. These results demonstrated that our clustering analysis accurately grouped the cells into different stages of differentiation and our identity assignments were correct.

Relationships between the clusters

To further examine the characteristics of the individual clusters, we performed gene enrichment analysis of the wild-type cells by comparing the expression profile of each cluster with those of all the other clusters and identified genes that were specifically

enriched in individual clusters. Using a cutoff of 1.80 fold as the minimum enrichment and an adjusted p value of 0.05, we identified a list of enriched genes for each cluster (Suppl. Table 5). The numbers of enriched genes in these clusters ranged from 126 to 686 with Cluster 6 having the most enriched genes (Suppl. Tables 5 and 6). The enriched genes further confirmed our initial cluster identity assignment, as many additional known marker genes specific for the cell states/types were enriched in the corresponding clusters (Suppl. Table 5). Examples of such genes included *Sfrp2*, *Sox2*, *Lhx2*, *Zfp36l1*, and *Vsx2* for RPCs (C0, C1, and C2) (Blackshaw et al., 2004; Gordon et al., 2013; Green et al., 2003; de Melo et al., 2016; Taranova et al., 2006), *Isl1*, *Nefl*, *Sncg*, *Gap43,* and *Ina* for RGCs (C5 and C6) (Mu et al., 2004, 2005a, 2008), *Thrb*, *Meis2*, *Prdm1*, and *Gngt2* for photoreceptors (C8 and C9) (Brzezinski et al., 2013; Ng et al., 2001; Rodgers et al., 2016; Trimarchi et al., 2007), *Tfap2a*, *Prdm13*, and *Onecut2* for amacrine and horizontal cell precursors (C7) (Bassett et al., 2012; Goodson et al., 2018; Sapkota et al., 2014), and *Ccnd2* and *Msx1* for ciliary margin cells (C10) (Bélanger et al., 2017, 2017; Marcucci et al., 2016).

Next, we examined the expression of the top ten enriched genes as ranked by p value from each wild-type cluster across all the clusters and represented the data by a heatmap (Figure 4A). This analysis did not only confirm their enrichment in the corresponding clusters but also revealed that many of these genes were expressed across several neighboring clusters, suggesting the relationships and continuity among these clusters along different developmental lineages. For example, the top ten enriched genes in C0 were also highly expressed in C1 and C2, indicating they indeed were all RPC clusters. The differences among these three clusters were likely due to their cell cycle status (Figure 3D), as many of the cluster-specific genes are directly involved in cell cycle regulation (Table 1, Suppl. Table 5). C3 and C4 were two other examples of this continuity. They continued to express many of RPC genes enriched in C0-C2, albeit at lower levels, but began to express such genes as *Atoh7*, *Dlx1*, *Dlx2*, *Neurod1*, and *Otx2* which regulate retinal cell differentiation (Brown et al., 2001; Nishida et al., 2003; Pennesi et al., 2003; Wang et al., 2001; Zhang et al., 2017). On the other hand, many of the genes in C3 and C4 trailed into the further differentiated clusters including C5 and C6 (RGCs), C7 (horizontal and amacrine cells), and C8 and C9 (photoreceptors), suggesting that C3 and C4 cells were intermediate transitional RPCs poised to differentiate (Figure 4A). Although C5 and C6 were both assigned as RGC clusters, C5 continued to express many genes enriched in C3 and C4, but C6 essentially stopped expressing them (Figure 4A). On the other hand, although C5 cells expressed the early RGC marker genes such as *Isl1* and *Pou4f2* at high levels, they had not or had just begun to express many of the RGC-specific genes encoding RGC structure and function proteins such as *Nefl*, *Sncg*, *Gap43*, *Nefm*, and *Ina*, but these genes were highly expressed C6 cells (Figure 4A). Thus, C5 cells were nascent RGCs and C6 were further differentiated RGCs. Similarly, C8 were nascent photoreceptors and C9 were more differentiated photoreceptors based on the expression of early and later photoreceptor marker genes (Figure 4A). As mentioned above, C7 cells were considered precursors for horizontal and amacrine cells as they expressed genes required for both lineages such as *Ptf1a* but more specific marker genes for the two cell

types were not robustly expressed yet. From these overlaps in expression the trajectories of the different cell lineages could be postulated, which all started from the naïve RPCs (C0, C1, C2), underwent the transitional RPCs (C3, C4), and finally reached the different terminal cell fates (C5-C9).

The unidirectional trajectories were further validated by examining the overlaps of all enriched gene lists in different clusters; there were significant overlaps between the naïve RPCs (C0-C3) and transitional RPCs (C3, C4), between the transitional RPCs (C3, C4) and the three terminal lineages including the RGC clusters C5 and C6, horizontal and amacrine cluster C7, photoreceptors clusters C8 and C9, but little overlap between the naïve RPCs and fate-committed neurons (Figure 4B, and data not shown), further confirming that C3 and C4 were in a transitional state linking naïve RPCs and differentiating neurons. Of note is that C10, which was composed of the ciliary margin cells with a unique gene signature, also expressed many of the genes enriched in RPC clusters C0-C3 (Figure 4A, Suppl Table 5), highlighting the close developmental relationship of the ciliary margin and the neural retina.

To further validate the relationships between the cells in these clusters, we also performed trajectory analysis using the SCANPY tool which is based on diffusion pseudotime (DPT) by measuring transitions between cells using diffusion-like random walks (Haghverdi et al., 2016). As shown in Figure 4C and consistent with the conclusions from the heatmap with the cluster-enriched genes, three definitive trajectories representing photoreceptors, horizontal cells and amacrine cells, and RGCs were clearly identified, which all originated from the transitional RPCs that were downstream of the naïve RPC clusters. Not surprisingly, being the first cell types to form, the RGC trajectory advanced the furthest (Figure 4C). All three trajectories also existed in the *Atoh7*-null cells (Figure 4D); whereas the other two trajectories were not affected, the RGC trajectory appeared to have progressed through C5 but stalled at C6, consistent with the fact that RGCs are specifically affected in the *Atoh7*-null retina.

Characteristics of individual cell states during retinal development.

To better understand the properties of the cell states/types represented by individual clusters, we further examined the biological function of the enriched genes in these clusters by DAVID GO analysis of each of these lists (Huang et al., 2009). For simplicity, we combined similar clusters, including C0 to C2 (naïve RPCs), C3 and C4 (transitional RPCs), C5 and C6 (RGCs), and C8 and C9 (photoreceptors) (Table 1). The top five GO biological processes enriched in naïve RPCs were cell cycle cell division, mitotic nuclear division, nucleosome assembly, and chromosome segregation, confirming that they were indeed actively dividing RPCs at different phases of the cell cycle (Table 1). Two of the top five GO terms associated with C3 and C4 included cell cycle and cell division, further implying they were still RPCs. Interestingly, the other three top GO terms were all associated with RNA processing (Table 1), indicating that this process plays a critical role in these transitional RPCs. In contrast, GO terms enriched in RGCs, horizontal and amacrine cells and photoreceptors were all related to the various aspect of neural

development and function, further confirming that their identities were correctly assigned and that the enriched genes were involved in their formation.

The enriched gene lists also included many genes with unknown expression patterns and functions in the retina. The information from our scRNA-seq analysis thus can potentially serve as a rich source to identify novel candidate genes in retinal development. To examine how faithful these enriched genes reflected their actual expression patterns in the developing retina, we chose genes from the enriched lists whose expression and function have not been well analyzed and compared their predicted expression patterns as presented by feature plots with that reported in the Eurexpress in situ hybridization database (Diez-Roux et al., 2011) (http://www.eurexpress.org/ee/). We found that the feature plots almost always correctly predicted the actual expression patterns, often with more details than in situ hybridization, as exemplified by 5 naïve RPC enriched genes and 10 RGC enriched genes whose expression and function in the retina have not been characterized (Suppl. Figures 2 and 3, Suppl. Table 5). Thus, the clustering data based on scRNA-seq analysis can serve as a very useful resource for identifying novel genes as markers or candidates for further functional analysis.

The scRNA-seq data also could be used to clarify contradicting results. For example, *Sox4* and *Sox11*, which encodes two transcription factors critical for RGC development (Chang et al., 2017; Jiang et al., 2013; Kuwajima et al., 2017), have been identified to be expressed mostly in RGCs, although there have been conflicting reports regarding whether they are also expressed in RPCs (Jiang et al., 2013; Kuwajima et al., 2017; Usui et al., 2013; Wu et al., 2015). In the *Atoh7*-null retina, since most RGCs are absent, it was indicated that *Sox4* and *Sox11* are downregulated (Jiang et al., 2013; Wu et al., 2015). However, we did not detect significant changes in conventional RNA-seq analysis (Suppl Table 5). These contradicting results were resolved by comparison of their expression in corresponding clusters from our single-cell RNA-seq data; both genes were extensively expressed in all the clusters (Figure 5A, B), but were at lowest levels in naive RPCs (C0-2), began to increase in the transitional RPCs (C3, C4), and reached the highest levels in differentiated neurons including RGCs (C5, C6) and amacrine and horizontal precursors (C7) (Figure 5C). These patterns were further confirmed by in situ hybridization with RNAscope probes (Wang et al., 2012) (Figure 5D, E). In the *Atoh7*-null retina, the overall patterns of *Sox4* and *Sox11* remained and the levels were comparable in all clusters, with only moderate upregulation of *Sox4* in differentiated RGCs (C6, Figure 5C). Therefore, despite the loss of RGCs, the overall expression levels of these two genes did not change in the *Atoh7*-null retina as detected by regular RNA-seq using total RNA from whole retinas. Nevertheless, as further discussed later, the differential expression levels of *Sox4* and *Sox11* along the differentiation trajectories may be related to their functions in the retina, particularly in RGC genesis.

Atoh7 marks a transient state shared by all early differentiation cell fates

Cells in C3 and C4 appeared to represent a critical transitional stage linking naïve RPCs and differentiating neurons along individual lineage trajectories. They were considered

RPCs since they still were in the cell cycle (Figure 3D, E), expressed many RPC marker genes (Figure 4A, B, Suppl. Table 5), and their fate was not committed (Figure 4C). Nevertheless, expression of many of the general RPC markers genes was significantly decreased in these cells (Figures 3C, 4A). Close examination indicated that these cells expressed many genes involved in specific cell lineages, including *Atoh7, Sox4, Sox11, Neurog2, Neurod1, Otx2, Onecut1, Foxn4, Ascl1, Olig2, Dlx1, Dlx2,* and *Bhlhe22* (Figure 6A and Suppl. Table 5). These genes have all been reported to be expressed in subsets of RPCs, and function in or mark specific lineages. For example, *Atoh7* and *Neurog2* are required for the RGC lineage (Brzezinski et al., 2012; Feng et al., 2010; Hufnagel et al., 2010), *Otx2* and *NeuroD1* functions in the photoreceptor lineage (Nishida et al., 2003; Pennesi et al., 2003), whereas *Olig2*-expressing cells give rise to cone and horizontal progenies (Hafler et al., 2012). *Onecut1* and *Onecut2* function in essentially all the early retinal cell lineages (Emerson et al., 2013; Sapkota et al., 2014). Other genes included *Foxn4* for horizontal and amacrine cells, *Dlx1* and *Dlx2* for RGCs and amacrine cells, and *Bhlhe22* (also known as *bHLHb5*) for amacrine cells and bipolar cells (Feng et al., 2006, 2011; Huang et al., 2014; Li et al., 2004; de Melo et al., 2005). The fact that these cells were clustered together and were enriched in these genes for different lineages indicated that they possessed shared properties. More interestingly, *Atoh7* was expressed in almost all cells in C3 and C4 and trailed into all three differentiating lineages (Figure 6A, C). Although this was consistent with previous findings that *Atoh7*-expressing cells are not fate-committed and can adopt all retinal fates (Brzezinski et al., 2012; Feng et al., 2010; Yang et al., 2003), the high percentage of transitional RPCs expressing *Atoh7* was a significant new finding. Moreover, several other factors including *Neurog2*, *Neurod1*, and *Otx2* were all expressed in substantial portions (>75%) of cells in this cluster (Figure 6A, C). Therefore, at least for these factors, although they regulate distinct lineages, their expression overlapped substantially in the transitional RPCs. However, as the trajectories of individual lineages progressed*, Neurod1* and *Otx2*, unlike *Atoh7*, became restricted to only the photoreceptor lineage (Figure 6C). As mentioned above, *Sox4* and *Sox11*, had elevated expression in the transitional RPCs (C3 and C4) and continued to be expressed in all lineages (Figure 5A-C). Nevertheless, other factors, such as *Olig2*, *Onecut1*, *Foxn4*, *Ascl1*, seemed to be expressed in considerably fewer transitional RPCs (Figure 6A). However, the overlaps between these genes could be more extensive as the percentage of gene expression in each cluster was likely underestimated due to sequence depth and expression levels. Nevertheless, it is very likely that the transitional RPCs remained heterogeneous.

Another prominent feature of the transitional RPCs is that many genes encoding components of the Notch pathway, including *Dll1*, *Dll3*, *Dll4*, *Notch1*, *Hes5*, *Hes6*, and *Mfng* were enriched, further emphasizing the critical roles this pathway plays in retinal development (Figure 6B, Suppl. Table 5). The expression of *Dll1*, *Dll3*, and *Dll4* was of particular interest; they all were only expressed highly in transitional RPCs (C3 and C4) and the differentiating clusters, but not much in the naïve RPC clusters. Although Hes5, one of the effector genes of the pathway, was enriched, *Hes1,* another downstream effector of the pathway, was significantly downregulated in C3 and C4, as compared to

the naïve RPCs (Suppl. Table 5 and data not shown), indicating that these two genes were differentially regulated and likely had both shared and distinct functions (Wall et al., 2009). These findings suggested that when selected RPCs were poised for differentiation and began to express *Atoh7* and genes for other fates, they also elevated the levels of ligands of the Notch pathway, which in turn modulate the Notch activities in the naïve RPCs. Likely this is part of the mechanism by which the balance between proliferation and differentiation is achieved.

Many additional genes, e.g. *Gadd45a*, *Btg2*, *Penk*, *Srrm4*, and *Plk1, Sstr2, and Ccnb1*, were enriched in the transitional RPCs (Figure 6B, Suppl. Table 5), but their roles are mostly unknown. For example, *Gadd45a* and *Btg2*, two genes involved in cell cycle arrest, DNA repair and apoptosis (Mao et al., 2015; Salvador et al., 2013; Tamura et al., 2012; Yuniati et al., 2019), were highly enriched in transitional RPCs, but they diverge in the differentiating lineages (Figure 6B). *Gadd45a* continued to be expressed in nascent RGCs (C5), whereas *Btg2* maintained its expression in photoreceptors (C8, C9) (Figure 6B). We further confirmed by RNAscope in situ hybridization that they each indeed were expressed in a subset of RPCs at different developmental stages examined (E12.5, E14.5, and E17.5), with patterns very similar to that of *Atoh7*. Both genes are responsive to stress-induced growth arrest and inhibit the G1/S progression in the cell cycle. Although their roles in retinal development have not been well studied, they likely participate in establishing the transitional cell state in these cells, which are primed to exit the cell cycle and commit to distinct cell fates.

These results indicated that all the early retinal cell fates go through a shared cell state which is characterized by downregulation of naïve RPC genes, upregulation of the Notch ligands, downregulation of the Notch pathway, and upregulation of neurogenic genes for various retinal fates. Of note is that, although *Atoh7* was expressed in essentially all transitional RPCs, deletion of *Atoh7* did not affect the formation of this cell state (Figure 3B), indicating that Atoh7 is not required for the establishment of this critical cell state in retinal development.

Cell cluster-specific changes in gene expression in the *Atoh7*-null retina

E13.5 *Atoh7*-null retinal cells could be grouped in the same overall 11 clusters as those from the wild-type retina, and corresponding clusters almost completely overlapped in the 2D projection of the UMAP analysis (Figure 3A, B). Most clusters, including the transitional RPCs (C3 and C4), contained comparable proportions of cells in the wild-type and mutant retinas (Suppl. Figure 4A). However, several clusters demonstrated marked changes. There was an about two-fold increase in the proportion of mutant C0 cells. Since most C0 cells were in G1/S of the cell cycle (Figure 2C, D), this may reflect the reduced proliferation of the naive RPCs caused by reduced Shh signaling and the G1/S cyclin (Cyclin D1) levels (Figure 2) (Brzezinski et al., 2012; Le et al., 2006; Mu et al., 2005a). The cell number in mutant C7 reduced almost by half, which is consistent with previous reports suggesting that Atoh7 plays a role in the genesis of horizontal cells (Brzezinski et al., 2012; Wu et al., 2015). There was also a noticeable drop in the number of nascent

photoreceptor cells (C8), but no change in the more differentiated photoreceptors (C9). The significance of this observation is not known. The mutant cluster with the most significant change was C6, which were differentiating RGCs, with an ~5 fold reduction as compared to the wild-type cluster (Suppl. Figure 4A). However, the nascent RGC cluster (C5) and the transitional RPC clusters (C3 and C4) did not show obvious changes in cell numbers. As discussed earlier, deletion of *Atoh7* did not substantially affect the overall cell cycle status of each cluster except for C0 as noted above, the relationships of the different clusters, or the overall trajectories of the distinct lineages (Figures 3A-E, 4C, D).

The same corresponding clusters observed in the *Atoh7*-null retina provided us the opportunity to probe the cell state/type-specific gene expression changes caused by deletion of *Atoh7*. Global gene expression between corresponding wild-type and *Atoh7*-null clusters were highly similar as revealed by the scatter plots; the correlation coefficients (R^2) ranged from 0.870 to 0.969 (Suppl. Figure 4B). The high R^2 values indicated that gene expression levels detected by scRNA-seq were highly robust and reproducible. They were also consistent with the knowledge that Atoh7 functions highly specifically in the RGC lineage. Accordingly, the two RGC clusters (C5 and C6) had the lowest R^2 values (0.875 and 0.870 respectively), as RGCs are the major cell type affected by *Atoh7* deletion. By comparing corresponding wild-type and *Atoh7*-null clusters, we identified a total of 1829 DEGs (Suppl. Tables 7-17). Comparison with the DEG list from conventional RNA-seq revealed an overlap of only 290 genes (Suppl. Tables 2, 7-17). Further examination of the none-overlapped genes indicated scRNA-seq could not effectively detect DEGs with relatively low expression levels. For example, *Shh* was readily detected as a DEG by regular RNA-seq, but not by scRNA-seq, although *Gli1*, the downstream target gene of the Shh pathway, was detected by both methods (Figure 2A, Suppl. Tables 2, 7, 8, 12, 13). This was likely due to the relatively low sequencing coverage of the transcriptome in scRNA-seq. Conventional RNA-seq, on the other hand, was inefficient in detecting DEGs that were expressed in multiple clusters but the change only occurs in selected clusters (see below). These results indicated that each method had limitations in identifying DEGs, particularly in tissues with complex cellular compositions, and that the two methods were complementary in determining a more complete picture of changes in gene expression.

Nevertheless, genes identified by comparing the corresponding wild-type and mutant clusters provided further insights into the function of Atoh7. Our focus will be on the DEGs in naïve RPCs (Suppl. Table 7-9), transitional RPCs (Suppl. Table 10, 11), and RGCs (Suppl. Table 12, 13), since they were directly related to RGC development, whereas only small numbers of DEGs were detected for other clusters (Suppl. Table 14-17). DEGs in the naïve clusters (C0-C2) were genes involved in the intrinsic properties and proliferation of RPCs, some of which included downregulated genes *Fgf15*, *Ccnd1*, *Gli1*, *Mcm7*, and *Hes1*. Since Atoh7 is not expressed in these cells (Figure 3C, Figure 6C), these DEGs were likely affected non-cell autonomously via the Notch and Shh pathways, highlighting the interaction between RGCs and RPCs. Key changes in the transitional RPCs (C3 and C4) included downregulation of *Dll3*, *Dlx2*, and *Eya2* and upregulation of *Sfrp2*, *Ebf1*,

Mybl1, and *Insm1*, although the significance of these changes is largely unknown. As expected, the largest number of DEGs were found between the wild-type and mutant RGC clusters (C5 and C6); 450 DEGs were found in C5, 618 DEGs were found in C6, and collectively a total of 861 DEGs were identified in these two clusters (Suppl. Table 12, 13). These genes likely are directly relevant to the establishment and maintenance of the RGC identity; among them included *Pou4f2* and *Isl1*, which are critical in establishing the lineage by activating many regulatory, functional and structural genes critical for RGC differentiation (Suppl. Table 2) (Mu et al., 2004, 2008; Pan et al., 2008; Wu et al., 2015).

The RGC lineage forms and advances substantially in the absence of Atoh7

The two clusters representing the RGC lineage (C5 and C6) were still present in the *Atoh7*-null retina (Figure 3B, Suppl. Figure 4A). Although a significant reduction in cell number was found in more differentiated RGCs (C6) as expected, no major change in the proportion of nascent RGCs (C5) was observed in the *Atoh7*-null retina, (Suppl. Figure 4A). Thus, the RGC lineage still formed initially, but the trajectory stalked prematurely (Figure 4C, D, Suppl. Figure 4A). These findings indicated that, contrary to previous conclusions (Brown et al., 2001; Wang et al., 2001), the RGC lineage still formed and advanced considerably in the absence of Atoh7, although the cell eventually failed to differentiate into fully functional RGCs.

To better understand the underlying genetic mechanisms for the defective RGC development in the *Atoh7*-null retina, we further examined the DEGs in C5 and C6 by comparing them (861 genes, Suppl. Table 12, 13) with the enriched genes in C5 and C6 (821 genes, Suppl. Table 5), which were mostly RGC-specific genes (Figure 7A). Although a significant portion of the C5/C6 enriched genes (386 genes) were downregulated as expected, many of them did not change in expression (405 genes). A small number of C5/C6-enriched genes (34 genes) were actually upregulated. On the other hand, many downregulated DEGs (198 genes) and most upregulated DEGs (246 genes) were not enriched in C5/C6. These findings suggested these genes were regulated in different modes with regard to the RGC lineage.

To further confirm these findings, we performed unsupervised clustering of all the 1266 genes included in the C5/C6 DEG list and enriched gene list across C3 to C6 of wild-type and *Atoh7*-null cells. This led to 7 groups of genes with distinct expression dynamics across the clusters, including RGC-enriched and downregulated (Group 1a, b); RGC-enriched but not significantly changed (Group 2); none RGC-enriched but upregulated (Group 3a, b); and none RGC-enriched but downregulated (Group 4a, b) (Figure 7B, only C3 to C6 are shown, and Suppl. Table 18). Example genes representing some of these distinct expression modes across different cell types/states were more clearly demonstrated by violin plots (Figure 7C). From these analyses, it was apparent that, as expected, a large proportion of RGC-specific genes, including *Pou4f2*, *Isl1*, *Syt4*, *Pou6f2*, *Gap43*, *Elavl4*, were downregulated in the *Atoh7*-null retina (Figure 7). Among them, some genes such as *Pou4f2* and *Syt4* exhibited little expression in the mutant, but other genes, such as *Isl1* (data not shown), *Pou6f2 Gap43*, *Elavle4*, were still expressed at

variable but substantial levels (Figure 7B, C). In addition, a substantial number of RGC genes such as *Nhlh2* remained expressed at similar levels as in the wild-type retina (Figure 7B, C). The remaining RGC-specific gene expression in the *Atoh7*-null retina, albeit often at lower levels, likely underlay the presence of nascent and differentiating RGCs.

Nevertheless, these RGCs were not normal, since they not only failed to express a large number of genes either completely or at sufficient levels, but also aberrantly overexpressed many genes not enriched in RGCs (Groups 3a, b in Figure 7B, Figure 7C). Some of these genes, e.g. *Kctd8* (Figure 7C), were expressed at low levels in all wild-type clusters but were significantly upregulated specifically in RGCs (Group 3a). Other genes expressed in naïve and transitional RPCs but not in RGCs in the wild-type retina remained expressed in the mutant RGCs (Group 3b). Among these genes, particularly worth noting is *Neurod1,* which is normally expressed in the transitional RPCs (C3 and C4) and photoreceptors (C8, and C9), but not in RGCs (C5 and C6) (Figure 6C, Figure 7C). In the *Atoh7*-null retina, although expression of *Neurod1* did not change in clusters where it normally was activated, it became highly overexpressed in RGCs (Figure 7C).

The collective dysregulation of genes in *Atoh7*-null cells likely led to the truncated RGC trajectory. These cells progressed to an RGC-like state by expressing many of the RGC genes, often at reduced levels, but also overexpressed many genes abnormally. Because of the aberrant gene expression, they failed to fully differentiate into more mature RGCs and most of them likely died (Feng et al., 2010).

Discussion

In this study, we first used regular RNA-seq to investigate the global transcriptomic changes in three mutant retinas, *Atoh7*-, *Pou4f2*-, and *Isl1*-null, during early development. The RNA-seq data provide a comprehensive list of genes expressed in the early developing retina (Suppl. Table 1). All genes known to function at this stage are on the list, and the gene list can be further mined for novel key regulators. Since all three mutants are defective in RGC development, this analysis provides a more complete picture and expands our knowledge of the function and hierarchical relationships of the three transcription factors in this lineage. The overlaps of downstream genes activated by the three factors confirm that Atoh7 acts upstream, whereas Pou4f2 and Isl1 are dependent on Atoh7 but only represent a part of the downstream events. As an example, the Shh pathway is downstream of all three factors and functions through complex feedback mechanisms to coordinate proliferation and differentiation. Nevertheless, many RGC-specific genes were only dependent on Atoh7, but not on Pou4f2 or Isl1, indicating other factors parallel to Pou4f2 and Isl1 are at work in the RGC lineage. On the other hand, the lists of upregulated genes, which are normally repressed by the three transcription factors, demonstrated that the three factors exert their repressive roles largely independently at two levels: Atoh7 in RPCs whereas Pou4f2 and Isl1 in RGCs, although significant cross-talk between the two levels exists.

We then performed scRNA-seq on E13.5 wild-type and *Atoh7*-null retinal cells. The analysis not only correctly identified known cell states/types present at the stage, but also identified enriched genes for each cluster. The cluster-specific expression provided precise expression information not available before, demonstrating the power of this technology. Specifically, genes enriched in different clusters from our scRNA-seq data define specific states along the developmental trajectories (Figure 8) and provide highly accurate information on their cell state/type-specific expression patterns (Figure 8). These results not only validate several recent reports of scRNA-seq analysis of both mouse and human retinas showing the presence of distinct lineage trajectories and a shared transitional but plastic (multipotent) cell state (transitional RPCs) by all the early trajectories (Clark et al., 2019; Giudice et al., 2019; Sridhar et al., 2020), but also significantly extend those findings by revealing that *Aoth7* is expressed in all transitional RPCs and highly overlaps with genes involved in lineages other than RGCs. Our study thus provides further insights into the nature of RPC competence for different retinal cell fates and the likely mechanism by which these fates are committed. Previous studies indicated that subsets of RPCs marked by specific genes exist and that these subsets are required for or biased toward particular cell fates (Brzezinski et al., 2011, 2012; Feng et al., 2010; Hafler et al., 2012). However, the relationship between these RPC subpopulations and its relevance to the competence of RPCs for different retinal fates have not been known. Our current study establishes that these populations highly overlap and can be considered as a shared cell state of all early retinal cell types (Figure 8). This state is characterized by co-expression of genes essential for individual retinal cell types, such as *Atoh7* and *Neurog2* for RGCs, *Otx2* and *Neurod1* for photoreceptors, and *Foxn4* and *Onecut1/2* for amacrine and horizontal cells. The commonality of these factors is that they function before fate commitment but promote RPCs toward individual lineages. The transitional RPCs, still dividing but likely in the last cell cycle(s) (Brzezinski et al., 2012; Feng et al., 2010; Fu et al., 2009; Le et al., 2006; Miesfeld et al., 2018; Yang et al., 2003), are also characterized by significantly reduced expression of the naïve RPC markers, increased expression of ligands for the Notch pathway, and decrease in the Notch pathway activities. These aspects of transition are likely coordinated, although the underlying mechanisms are not known. The Notch pathway is essential for RPC proliferation but inhibits differentiation (Austin et al., 1995; Jadhav et al., 2006; Maurer et al., 2014; Perron and Harris, 2000; Riesenberg et al., 2009; Yaron et al., 2006). Promotion of proliferation by Notch may be achieved through interaction with some of the naïve RPC genes such as *Sox2*, *Lhx2*, and *Pax6* (Furukawa et al., 2000; Lee et al., 2005; de Melo et al., 2016; Taranova et al., 2006). Consistently, retinal cell differentiation requires the downregulation of the Notch pathway (Austin et al., 1995; Nelson et al., 2006, 2007; Perron and Harris, 2000). Thus, downregulation of the Notch pathway likely is a key step for establishing this transitional state, and upregulation of the Notch ligands and other components may serve as a mechanism to balance proliferation and differentiation by lateral inhibition (Cau and Blader, 2009; Kageyama et al., 2008; Lathia et al., 2008). This downregulation is likely mediated in part by transcription factors like Atoh7, Ascl1, and Foxn4 (Luo et al., 2012; Nelson et al., 2006, 2009). Additional genes, such as *Gadd45a*,

Btg2, *Penk*, *Srrm4*, *Plk1, Sstr2, and Ccnb1*, were found highly expressed in this transitional state; they likely also play key roles in the transition from naïve RPCs to transitional RPCs.

Since all early cell types arise from these transitional RPCs, as suggested by our trajectory analysis, the long-postulated RPC competence for retinal cell fates may be determined and defined by the genes expressed in them. For example, their competence for the RGC fate is dictated at least in part by *Atoh7*, whose expression coincides with RGC production (Brown et al., 1998; Fu et al., 2009). At later stages, when *Atoh7* is not expressed, RPCs lose their competence for the RGC fate. Consistent with the idea, deletion of *Atoh7* does not affect the establishment of this transitional state or the competences for other cell types. Since key regulators of different fates are co-expressed in these transitional RPCs, an outstanding question that arises is how the eventual outcome, i.e. adopting one particular fate versus another, is achieved. The mechanisms by which Atoh7 promotes the RGC fate may serve as a point of discussion regarding how transitional RPCs take on a specific developmental trajectory. In agreement with previous findings that Atoh7 is essential but not sufficient for the RGC lineage, we observed that *Atoh7* is expressed in all transitional RPCs and its expression trails into all three lineages being generated at E13.5. Since Atoh7 is expressed in all transitional RPCs and thus significantly overlap with competent factors for other fates (e.g. Neurod1 and Otx2 for photoreceptors), these factors likely compete with each other to steer the transitional RPCs toward different directions (Figure 8). The competition may occur at transcription level through cross-repression as evidenced by the upregulation in the *Atoh7*-null retina of *Neurod1* and *Bhlhe22*, which are required for photoreceptors and amacrine cells respectively. However, this may not be the only or even the dominant mechanism, as most other genes including *Otx2* expressed in the transitional RPCs are not affected by the loss of Atoh7. Atoh7 and the other competence factors may compete with each other stochastically by activating distinct sets of downstream genes essential for the respective fates, e.g. *Pou4f2* and *Isl1* for the RGCs, *Ptf1a* for horizontal and amacrine cells, and *Crx* for photoreceptors. This idea is consistent with previous observations that RPCs generated different retinal cell types in a stochastic fashion (Cayouette et al., 2003; Gomes et al., 2011). Nevertheless, the eventual outcome is likely determined genetically; the proportion of different cell types produced at any given time is likely dictated by the presence of the competence factors and their relative activities. This idea is further supported by the finding that *Atoh7* gene dosage affects the number of RGCs produced (Prasov et al., 2012). Activities of these transcription factors may also be modified postranslationally (Ali et al., 2011; Moore et al., 2002; Satou et al., 2018; Tomic et al., 2018). On the other hand, the transitional RPCs are still heterogeneous, as indicated by the uneven expression of many genes in these cells. This has also been demonstrated by lineage-tracing experiments; although *Olig2*, *Neurog2*, and *Ascl1* are all expressed in transitional RPCs, cells expressing these genes are biased in producing specific retinal progenies (Brzezinski et al., 2011; Hafler et al., 2012). The heterogeneity of transitional RPCs may reflect their progression toward different developmental trajectories.

Our scRNA-seq analysis on the *Atoh7*-null retina leads to significant insights into RGC development by identifying specific changes in gene expression through both direct and indirect mechanisms. Of particular significance was our observation that in the absence of Atoh7, the RGC trajectory still progressed considerably but stalked prematurely. This may have been observed previously but not fully appreciated; many of the mutant Atoh7-expressing cells, marked by knock-in lacZ or Cre-activated reporter markers, still migrate to the inner side where RGCs normally reside (Brown et al., 2001; Brzezinski et al., 2012; Wang et al., 2001; Yang et al., 2003), but most of them likely die by apoptosis (Feng et al., 2010). However, the status of these cells has not been well characterized. Our results indicate that these cells are on the RGC trajectory, and many, but not all, RGC-specific genes are activated in them, although often not to the wild-type levels. These observations are in contrast to the previous conclusion that the RGC lineage does not form in the *Atoh7*-null retina and the mutant Atoh7-expressing cells simply take others fates. This new finding suggests that additional factor(s) other than Atoh7 function in the transitional RPCs to promote them toward the RGC lineage. We propose that the SoxC family of transcription factors, including Sox4 and Sox11, fulfill this role (Figure 8). This is based on previous reports that deletion of the SoxC genes leads to severely compromised RGC production (Chang et al., 2017; Jiang et al., 2013; Kuwajima et al., 2017), and our finding that they are expressed at high levels in the transitional RPCs and that their expression is not dependent on Atoh7. The SoxC factors likely also function in differentiating RGCs and other cell types, as they continue to be expressed in fate-committed retinal neurons. Thus, activation of early RGC genes such as *Pou4f2* and *Isl1*, likely requires both upstream inputs, but in the absence of Atoh7, the SoxC factors still activate some of the RGC genes (Figure 8). Ectopic expression of Pou4f2 and Isl1 together rescues RGC formation caused by deletion of *Atoh7*, and the two factors were proposed to be part of a core group of factors determining the RGC fate (Wu et al., 2015). In light of our current findings, the determination of the RGC fate is likely a gradual process over a time window without a clear boundary, and the function of Pou4f2 and Isl1 is to stabilize the developmental trajectory by activating genes essential for RGC differentiation and repressing genes for other fates. Some of the RGC genes are activated already by Atoh7 and/or other factors independent of Pou4f2 and Isl1, but require Pou4f2 and Isl1 to reach full amplitudes of expression, whereas many other RGC genes can only be activated by Pou4f2 and Isl1 (Figure 8).

Our study also demonstrates that regular RNA-seq and scRNA-seq complement each other and can be used in combination to provide much richer information regarding transcriptomic changes due to genetic perturbations. Although regular RNA-seq lacks cellular resolution, it is more sensitive in detecting genes expressed at low levels and/or in a smaller number of cells. On the other hand, scRNA-seq enables classification of cell states/types in complex tissues and provides insights into relationships among the different cell states/types. scRNA-seq also provides precise information regarding changes in gene expression in specific cell states/types. It is worth noting that, currently, likely due to limitations of sequence depth and library construction, genes expressed at

low levels and/or in small numbers of cells are not always readily detectable by scRNA-seq, but this may change as the technology further matures.

In summary, we used RNA-seq and scRNA-seq to survey gene expression in the developing retina and identify changes associated with deletion of key transcription factor genes for the RGC lineage. Our results provide a global view of the gene expression, cell states and their relationships in early retinal development. Furthermore, our study validates and further defines a transitional state shared by all early retinal cell fates (Figure 8). Atoh7, likely in collaboration with other factors, functions within this cell state to shepherd RPCs to the RGC lineage by competing with other lineage factors and activating RGC-specific genes. Further analysis of the shifts in the epigenetic landscape along individual trajectories in both wild-type and mutant retinas will help elucidate the underlying mechanisms of RGC differentiation.

Acknowledgments

We thank other members of the Mu laboratory and members of the Department of Ophthalmology and the Developmental Genomics Group, University of Buffalo, for helpful discussions. We also would like to thank Andrew Kelly technical support. The knock-in mouse lines were created by the Gene Targeting and Transgenic Resource Core at the Roswell Park Cancer Institute. Construction and sequencing of RNA-seq and scRNA-seq libraries were carried out at the Genomics and Bioinformatics Core of University at Buffalo. This project was supported by a National Eye Institute Grant (EY020545) to X.M.

References:

Akagi, T., Inoue, T., Miyoshi, G., Bessho, Y., Takahashi, M., Lee, J.E., Guillemot, F., and Kageyama, R. (2004). Requirement of multiple basic helix-loop-helix genes for retinal neuronal subtype specification. J Biol Chem *279*, 28492–28498.

Ali, F., Hindley, C., McDowell, G., Deibler, R., Jones, A., Kirschner, M., Guillemot, F., and Philpott, A. (2011). Cell cycle-regulated multi-site phosphorylation of Neurogenin 2 coordinates cell cycling with differentiation during neurogenesis. Dev. Camb. Engl. *138*, 4267–4277.

Austin, C.P., Feldman, D.E., Ida, J.A., Jr., and Cepko, C.L. (1995). Vertebrate retinal ganglion cells are selected from competent progenitors by the action of Notch. Development *121*, 3637–3650.

Bassett, E.A., and Wallace, V.A. (2012). Cell fate determination in the vertebrate retina. Trends Neurosci *35*, 565–573.

Bassett, E.A., Korol, A., Deschamps, P.A., Buettner, R., Wallace, V.A., Williams, T., and West-Mays, J.A. (2012). Overlapping expression patterns and redundant roles for AP-2 transcription factors in the developing mammalian retina. Dev Dyn *241*, 814–829.

Bélanger, M.-C., Robert, B., and Cayouette, M. (2017). Msx1-Positive Progenitors in the Retinal Ciliary Margin Give Rise to Both Neural and Non-neural Progenies in Mammals. Dev. Cell *40*, 137–150.

Belecky-Adams, T., Cook, B., and Adler, R. (1996). Correlations between terminal mitosis and differentiated fate of retinal precursor cells in vivo and in vitro: analysis with the “window-labeling” technique. Dev Biol *178*, 304–315.

Blackshaw, S., Harpavat, S., Trimarchi, J., Cai, L., Huang, H., Kuo, W.P., Weber, G., Lee, K., Fraioli, R.E., Cho, S.H., et al. (2004). Genomic analysis of mouse retinal development. PLoS Biol *2*, E247.

Brown, N.L., Kanekar, S., Vetter, M.L., Tucker, P.K., Gemza, D.L., and Glaser, T. (1998). Math5 encodes a murine basic helix-loop-helix transcription factor expressed during early stages of retinal neurogenesis. Development *125*, 4821–4833.

Brown, N.L., Patel, S., Brzezinski, J., and Glaser, T. (2001). Math5 is required for retinal ganglion cell and optic nerve formation. Development *128*, 2497–2508.

Brzezinski, J.A. th, Kim, E.J., Johnson, J.E., and Reh, T.A. (2011). Ascl1 expression defines a subpopulation of lineage-restricted progenitors in the mammalian retina. Development *138*, 3519–3531.

Brzezinski, J.A. th, Prasov, L., and Glaser, T. (2012). Math5 defines the ganglion cell competence state in a subpopulation of retinal progenitor cells exiting the cell cycle. Dev Biol *365*, 395–413.

Brzezinski, J.A. th, Uoon Park, K., and Reh, T.A. (2013). Blimp1 (Prdm1) prevents re-specification of photoreceptors into retinal bipolar cells by restricting competence. Dev Biol *384*, 194–204.

Calera, M.R., Topley, H.L., Liao, Y., Duling, B.R., Paul, D.L., and Goodenough, D.A. (2006). Connexin43 is required for production of the aqueous humor in the murine eye. J. Cell Sci. *119*, 4510–4519.

Cau, E., and Blader, P. (2009). Notch activity in the nervous system: to switch or not switch? Neural Develop. *4*, 36.

Cayouette, M., Barres, B.A., and Raff, M. (2003). Importance of intrinsic mechanisms in cell fate decisions in the developing rat retina. Neuron *40*, 897–904.

Cepko, C. (2014). Intrinsically different retinal progenitor cells produce specific types of progeny. Nat Rev Neurosci *15*, 615–627.

Cepko, C.L., Austin, C.P., Yang, X., Alexiades, M., and Ezzeddine, D. (1996). Cell fate determination in the vertebrate retina. Proc Natl Acad Sci U A *93*, 589–595.

Chang, K.-C., Hertz, J., Zhang, X., Jin, X.-L., Shaw, P., Derosa, B.A., Li, J.Y., Venugopalan, P., Valenzuela, D.A., Patel, R.D., et al. (2017). Novel Regulatory Mechanisms for the SoxC Transcriptional Network Required for Visual Pathway Development. J. Neurosci. Off. J. Soc. Neurosci. *37*, 4967–4981.

Clark, B.S., Stein-O'Brien, G.L., Shiau, F., Cannon, G.H., Davis-Marcisak, E., Sherman, T., Santiago, C.P., Hoang, T.V., Rajaii, F., James-Esposito, R.E., et al. (2019). Single-Cell RNA-Seq Analysis of Retinal Development Identifies NFI Factors as Regulating Mitotic Exit and Late-Born Cell Specification. Neuron *102*, 1111-1126.e5.

Diez-Roux, G., Banfi, S., Sultan, M., Geffers, L., Anand, S., Rozado, D., Magen, A., Canidio, E., Pagani, M., Peluso, I., et al. (2011). A High-Resolution Anatomical Atlas of the Transcriptome in the Mouse Embryo. PLoS Biol. *9*.

Dobin, A., Davis, C.A., Schlesinger, F., Drenkow, J., Zaleski, C., Jha, S., Batut, P., Chaisson, M., and Gingeras, T.R. (2013). STAR: ultrafast universal RNA-seq aligner. Bioinformatics *29*, 15–21.

Emerson, M.M., Surzenko, N., Goetz, J.J., Trimarchi, J., and Cepko, C.L. (2013). Otx2 and Onecut1 promote the fates of cone photoreceptors and horizontal cells and repress rod photoreceptors. Dev Cell *26*, 59–72.

Erkman, L., McEvilly, R.J., Luo, L., Ryan, A.K., Hooshmand, F., O'Connell, S.M., Keithley, E.M., Rapaport, D.H., Ryan, A.F., and Rosenfeld, M.G. (1996). Role of transcription factors Brn-3.1 and Brn-3.2 in auditory and visual system development. Nature *381*, 603–606.

Feng, L., Xie, X., Joshi, P.S., Yang, Z., Shibasaki, K., Chow, R.L., and Gan, L. (2006). Requirement for Bhlhb5 in the specification of amacrine and cone bipolar subtypes in mouse retina. Development *133*, 4815–4825.

Feng, L., Xie, Z.H., Ding, Q., Xie, X., Libby, R.T., and Gan, L. (2010). MATH5 controls the acquisition of multiple retinal cell fates. Mol Brain *3*, 36.

Feng, L., Eisenstat, D.D., Chiba, S., Ishizaki, Y., Gan, L., and Shibasaki, K. (2011). Brn-3b inhibits generation of amacrine cells by binding to and negatively regulating DLX1/2 in developing retina. Neuroscience *195*, 9–20.

Fu, X., Kiyama, T., Li, R., Russell, M., Klein, W.H., and Mu, X. (2009). Epitope-tagging Math5 and Pou4f2: new tools to study retinal ganglion cell development in the mouse. Dev Dyn *238*, 2309–2317.

Fujitani, Y., Fujitani, S., Luo, H., Qiu, F., Burlison, J., Long, Q., Kawaguchi, Y., Edlund, H., MacDonald, R.J., Furukawa, T., et al. (2006). Ptf1a determines horizontal and amacrine cell fates during mouse retinal development. Development *133*, 4439–4450.

Furukawa, T., Morrow, E.M., and Cepko, C.L. (1997). Crx, a novel otx-like homeobox gene, shows photoreceptor-specific expression and regulates photoreceptor differentiation. Cell *91*, 531–541.

Furukawa, T., Mukherjee, S., Bao, Z.Z., Morrow, E.M., and Cepko, C.L. (2000). rax, Hes1, and notch1 promote the formation of Muller glia by postnatal retinal progenitor cells. Neuron *26*, 383–394.

Gan, L., Xiang, M., Zhou, L., Wagner, D.S., Klein, W.H., and Nathans, J. (1996). POU domain factor Brn-3b is required for the development of a large set of retinal ganglion cells. Proc Natl Acad Sci U A *93*, 3920–3925.

Gan, L., Wang, S.W., Huang, Z., and Klein, W.H. (1999). POU domain factor Brn-3b is essential for retinal ganglion cell differentiation and survival but not for initial cell fate specification. Dev Biol *210*, 469–480.

Giudice, Q.L., Leleu, M., Manno, G.L., and Fabre, P.J. (2019). Single-cell transcriptional logic of cell-fate specification and axon guidance in early-born retinal neurons. Development *146*, dev178103.

Gomes, F.L., Zhang, G., Carbonell, F., Correa, J.A., Harris, W.A., Simons, B.D., and Cayouette, M. (2011). Reconstruction of rat retinal progenitor cell lineages in vitro reveals a surprising degree of stochasticity in cell fate decisions. Development *138*, 227–235.

Goodson, N.B., Nahreini, J., Randazzo, G., Uruena, A., Johnson, J.E., and Brzezinski, J.A. (2018). Prdm13 is required for Ebf3+ amacrine cell formation in the retina. Dev. Biol. *434*, 149–163.

Gordon, P.J., Yun, S., Clark, A.M., Monuki, E.S., Murtaugh, L.C., and Levine, E.M. (2013). Lhx2 balances progenitor maintenance with neurogenic output and promotes competence state progression in the developing retina. J Neurosci *33*, 12197–12207.

Green, E.S., Stubbs, J.L., and Levine, E.M. (2003). Genetic rescue of cell number in a mouse model of microphthalmia: interactions between Chx10 and G1-phase cell cycle regulators. Development *130*, 539–552.

Hafler, B.P., Surzenko, N., Beier, K.T., Punzo, C., Trimarchi, J.M., Kong, J.H., and Cepko, C.L. (2012). Transcription factor Olig2 defines subpopulations of retinal progenitor cells biased toward specific cell fates. Proc Natl Acad Sci U A *109*, 7882–7887.

Haghverdi, L., Büttner, M., Wolf, F.A., Buettner, F., and Theis, F.J. (2016). Diffusion pseudotime robustly reconstructs lineage branching. Nat. Methods *13*, 845–848.

Huang, D.W., Sherman, B.T., and Lempicki, R.A. (2009). Bioinformatics enrichment tools: paths toward the comprehensive functional analysis of large gene lists. Nucleic Acids Res. *37*, 1–13.

Huang, L., Hu, F., Feng, L., Luo, X.-J., Liang, G., Zeng, X.-Y., Yi, J.-L., and Gan, L. (2014). Bhlhb5 is required for the subtype development of retinal amacrine and bipolar cells in mice. Dev. Dyn. Off. Publ. Am. Assoc. Anat. *243*, 279–289.

Hufnagel, R.B., Le, T.T., Riesenberg, A.L., and Brown, N.L. (2010). Neurog2 controls the leading edge of neurogenesis in the mammalian retina. Dev Biol *340*, 490–503.

Jadhav, A.P., Cho, S.H., and Cepko, C.L. (2006). Notch activity permits retinal cells to progress through multiple progenitor states and acquire a stem cell property. Proc Natl Acad Sci U A *103*, 18998–19003.

Jiang, Y., Ding, Q., Xie, X., Libby, R.T., Lefebvre, V., and Gan, L. (2013). Transcription factors SOX4 and SOX11 function redundantly to regulate the development of mouse retinal ganglion cells. J Biol Chem *288*, 18429–18438.

Kageyama, R., Ohtsuka, T., Shimojo, H., and Imayoshi, I. (2008). Dynamic Notch signaling in neural progenitor cells and a revised view of lateral inhibition. Nat. Neurosci. *11*, 1247–1251.

Kiyama, T., Mao, C.A., Cho, J.H., Fu, X., Pan, P., Mu, X., and Klein, W.H. (2011). Overlapping spatiotemporal patterns of regulatory gene expression are required for neuronal progenitors to specify retinal ganglion cell fate. Vis. Res *51*, 251–259.

Kuwajima, T., Soares, C.A., Sitko, A.A., Lefebvre, V., and Mason, C. (2017). SoxC Transcription Factors Promote Contralateral Retinal Ganglion Cell Differentiation and Axon Guidance in the Mouse Visual System. Neuron *93*, 1110-1125.e5.

La Torre, A., Georgi, S., and Reh, T.A. (2013). Conserved microRNA pathway regulates developmental timing of retinal neurogenesis. Proc Natl Acad Sci U A *110*, E2362-70.

La Vail, M.M., Rapaport, D.H., and Rakic, P. (1991). Cytogenesis in the monkey retina. J Comp Neurol *309*, 86–114.

Lathia, J.D., Mattson, M.P., and Cheng, A. (2008). Notch: From Neural Development to Neurological Disorders. J. Neurochem. *107*, 1471–1481.

Le, T.T., Wroblewski, E., Patel, S., Riesenberg, A.N., and Brown, N.L. (2006). Math5 is required for both early retinal neuron differentiation and cell cycle progression. Dev Biol *295*, 764–778.

Lee, H.Y., Wroblewski, E., Philips, G.T., Stair, C.N., Conley, K., Reedy, M., Mastick, G.S., and Brown, N.L. (2005). Multiple requirements for Hes 1 during early eye formation. Dev Biol *284*, 464–478.

Li, S., Mo, Z., Yang, X., Price, S.M., Shen, M.M., and Xiang, M. (2004). Foxn4 controls the genesis of amacrine and horizontal cells by retinal progenitors. Neuron *43*, 795–807.

Livesey, F.J., and Cepko, C.L. (2001). Vertebrate neural cell-fate determination: lessons from the retina. Nat Rev Neurosci *2*, 109–118.

Lukowski, S.W., Lo, C.Y., Sharov, A.A., Nguyen, Q., Fang, L., Hung, S.S., Zhu, L., Zhang, T., Grünert, U., Nguyen, T., et al. (2019). A single-cell transcriptome atlas of the adult human retina. EMBO J. e100811.

Luo, H., Jin, K., Xie, Z., Qiu, F., Li, S., Zou, M., Cai, L., Hozumi, K., Shima, D.T., and Xiang, M. (2012). Forkhead box N4 (Foxn4) activates Dll4-Notch signaling to suppress photoreceptor cell fates of early retinal progenitors. Proc. Natl. Acad. Sci. U. S. A. *109*, E553-562.

Macosko, E.Z., Basu, A., Satija, R., Nemesh, J., Shekhar, K., Goldman, M., Tirosh, I., Bialas, A.R., Kamitaki, N., Martersteck, E.M., et al. (2015). Highly Parallel Genome-wide Expression Profiling of Individual Cells Using Nanoliter Droplets. Cell *161*, 1202–1214.

Mao, B., Zhang, Z., and Wang, G. (2015). BTG2: A rising star of tumor suppressors (Review). Int. J. Oncol. *46*, 459–464.

Marcucci, F., Murcia-Belmonte, V., Wang, Q., Coca, Y., Ferreiro-Galve, S., Kuwajima, T., Khalid, S., Ross, M.E., Mason, C., and Herrera, E. (2016). The Ciliary Margin Zone of the Mammalian Retina Generates Retinal Ganglion Cells. Cell Rep. *17*, 3153–3164.

Mattar, P., Ericson, J., Blackshaw, S., and Cayouette, M. (2015). A conserved regulatory logic controls temporal identity in mouse neural progenitors. Neuron *85*, 497–504.

Maurer, K.A., Riesenberg, A.N., and Brown, N.L. (2014). Notch signaling differentially regulates Atoh7 and Neurog2 in the distal mouse retina. Development *141*, 3243–3254.

de Melo, J., Du, G., Fonseca, M., Gillespie, L.-A., Turk, W.J., Rubenstein, J.L.R., and Eisenstat, D.D. (2005). Dlx1 and Dlx2 function is necessary for terminal differentiation and survival of late-born retinal ganglion cells in the developing mouse retina. Dev. Camb. Engl. *132*, 311–322.

de Melo, J., Zibetti, C., Clark, B.S., Hwang, W., Miranda-Angulo, A.L., Qian, J., and Blackshaw, S. (2016). Lhx2 Is an Essential Factor for Retinal Gliogenesis and Notch Signaling. J Neurosci *36*, 2391–2405.

Menon, M., Mohammadi, S., Davila-Velderrain, J., Goods, B.A., Cadwell, T.D., Xing, Y., Stemmer-Rachamimov, A., Shalek, A.K., Love, J.C., Kellis, M., et al. (2019). Single-cell transcriptomic atlas of the human retina identifies cell types associated with age-related macular degeneration. Nat. Commun. *10*, 1–9.

Miesfeld, J.B., Glaser, T., and Brown, N.L. (2018). The dynamics of native Atoh7 protein expression during mouse retinal histogenesis, revealed with a new antibody. Gene Expr. Patterns GEP *27*, 114–121.

Moore, K.B., Schneider, M.L., and Vetter, M.L. (2002). Posttranslational mechanisms control the timing of bHLH function and regulate retinal cell fate. Neuron *34*, 183–195.

Mu, X., Beremand, P.D., Zhao, S., Pershad, R., Sun, H., Scarpa, A., Liang, S., Thomas, T.L., and Klein, W.H. (2004). Discrete gene sets depend on POU domain transcription factor Brn3b/Brn-3.2/POU4f2 for their expression in the mouse embryonic retina. Development *131*, 1197–1210.

Mu, X., Fu, X., Sun, H., Beremand, P.D., Thomas, T.L., and Klein, W.H. (2005a). A gene network downstream of transcription factor Math5 regulates retinal progenitor cell competence and ganglion cell fate. Dev Biol *280*, 467–481.

Mu, X., Fu, X., Sun, H., Liang, S., Maeda, H., Frishman, L.J., and Klein, W.H. (2005b). Ganglion cells are required for normal progenitor- cell proliferation but not cell-fate determination or patterning in the developing mouse retina. Curr Biol *15*, 525–530.

Mu, X., Fu, X., Beremand, P.D., Thomas, T.L., and Klein, W.H. (2008). Gene regulation logic in retinal ganglion cell development: Isl1 defines a critical branch distinct from but overlapping with Pou4f2. Proc Natl Acad Sci U A *105*, 6942–6947.

Nakhai, H., Sel, S., Favor, J., Mendoza-Torres, L., Paulsen, F., Duncker, G.I., and Schmid, R.M. (2007). Ptf1a is essential for the differentiation of GABAergic and glycinergic amacrine cells and horizontal cells in the mouse retina. Development *134*, 1151–1160.

Nelson, B.R., Gumuscu, B., Hartman, B.H., and Reh, T.A. (2006). Notch activity is downregulated just prior to retinal ganglion cell differentiation. Dev Neurosci *28*, 128–141.

Nelson, B.R., Hartman, B.H., Georgi, S.A., Lan, M.S., and Reh, T.A. (2007). Transient inactivation of Notch signaling synchronizes differentiation of neural progenitor cells. Dev. Biol. *304*, 479–498.

Nelson, B.R., Hartman, B.H., Ray, C.A., Hayashi, T., Bermingham-McDonogh, O., and Reh, T.A. (2009). Acheate-scute like 1 (Ascl1) is required for normal delta-like (Dll) gene expression and notch signaling during retinal development. Dev. Dyn. Off. Publ. Am. Assoc. Anat. *238*, 2163–2178.

Ng, L., Hurley, J.B., Dierks, B., Srinivas, M., Salto, C., Vennstrom, B., Reh, T.A., and Forrest, D. (2001). A thyroid hormone receptor that is required for the development of green cone photoreceptors. Nat Genet *27*, 94–98.

Nishida, A., Furukawa, A., Koike, C., Tano, Y., Aizawa, S., Matsuo, I., and Furukawa, T. (2003). Otx2 homeobox gene controls retinal photoreceptor cell fate and pineal gland development. Nat Neurosci *6*, 1255–1263.

Pan, L., Deng, M., Xie, X., and Gan, L. (2008). ISL1 and BRN3B co-regulate the differentiation of murine retinal ganglion cells. Development *135*, 1981–1990.

Pennesi, M.E., Cho, J.H., Yang, Z., Wu, S.H., Zhang, J., Wu, S.M., and Tsai, M.J. (2003). BETA2/NeuroD1 null mice: a new model for transcription factor-dependent photoreceptor degeneration. J Neurosci *23*, 453–461.

Perron, M., and Harris, W.A. (2000). Determination of vertebrate retinal progenitor cell fate by the Notch pathway and basic helix-loop-helix transcription factors. Cell Mol Life Sci *57*, 215–223.

Prasov, L., Nagy, M., Rudolph, D.D., and Glaser, T. (2012). Math5 (Atoh7) gene dosage limits retinal ganglion cell genesis. Neuroreport *23*, 631–634.

Qiu, F., Jiang, H., and Xiang, M. (2008). A comprehensive negative regulatory program controlled by Brn3b to ensure ganglion cell specification from multipotential retinal precursors. J Neurosci *28*, 3392–3403.

Rapaport, D.H., Wong, L.L., Wood, E.D., Yasumura, D., and LaVail, M.M. (2004). Timing and topography of cell genesis in the rat retina. J Comp Neurol *474*, 304–324.

Reh, T.A., and Kljavin, I.J. (1989). Age of differentiation determines rat retinal germinal cell phenotype: induction of differentiation by dissociation. J Neurosci *9*, 4179–4189.

Rheaume, B.A., Jereen, A., Bolisetty, M., Sajid, M.S., Yang, Y., Renna, K., Sun, L., Robson, P., and Trakhtenberg, E.F. (2018). Single cell transcriptome profiling of retinal ganglion cells identifies cellular subtypes. Nat. Commun. *9*, 2759.

Riesenberg, A.N., Liu, Z., Kopan, R., and Brown, N.L. (2009). Rbpj cell autonomous regulation of retinal ganglion cell and cone photoreceptor fates in the mouse retina. J Neurosci *29*, 12865–12877.

Robinson, M.D., McCarthy, D.J., and Smyth, G.K. (2010). edgeR: a Bioconductor package for differential expression analysis of digital gene expression data. Bioinformatics *26*, 139–140.

Rodgers, H.M., Belcastro, M., Sokolov, M., and Mathers, P.H. (2016). Embryonic markers of cone differentiation.

Salvador, J.M., Brown-Clay, J.D., and Fornace, A.J. (2013). Gadd45 in stress signaling, cell cycle control, and apoptosis. Adv. Exp. Med. Biol. *793*, 1–19.

Sapkota, D., Chintala, H., Wu, F., Fliesler, S.J., Hu, Z., and Mu, X. (2014). Onecut1 and Onecut2 redundantly regulate early retinal cell fates during development. Proc Natl Acad Sci U A *111*, E4086-95.

Satou, Y., Minami, K., Hosono, E., Okada, H., Yasuoka, Y., Shibano, T., Tanaka, T., and Taira, M. (2018). Phosphorylation states change Otx2 activity for cell proliferation and patterning in the Xenopus embryo. Dev. Camb. Engl. *145*.

Shekhar, K., Lapan, S.W., Whitney, I.E., Tran, N.M., Macosko, E.Z., Kowalczyk, M., Adiconis, X., Levin, J.Z., Nemesh, J., Goldman, M., et al. (2016). Comprehensive Classification of Retinal Bipolar Neurons by Single-Cell Transcriptomics. Cell *166*, 1308-1323.e30.

Sridhar, A., Hoshino, A., Finkbeiner, C.R., Chitsazan, A., Dai, L., Haugan, A.K., Eschenbacher, K.M., Jackson, D.L., Trapnell, C., Bermingham-McDonogh, O., et al. (2020). Single-Cell Transcriptomic Comparison of Human Fetal Retina, hPSC-Derived Retinal Organoids, and Long-Term Retinal Cultures. Cell Rep. *30*, 1644-1659.e4.

Stuart, T., Butler, A., Hoffman, P., Hafemeister, C., Papalexi, E., Mauck, W.M., Hao, Y., Stoeckius, M., Smibert, P., and Satija, R. (2019). Comprehensive Integration of Single-Cell Data. Cell *177*, 1888-1902.e21.

Swaroop, A., Kim, D., and Forrest, D. (2010). Transcriptional regulation of photoreceptor development and homeostasis in the mammalian retina. Nat Rev Neurosci *11*, 563–576.

Tamura, R.E., de Vasconcellos, J.F., Sarkar, D., Libermann, T.A., Fisher, P.B., and Zerbini, L.F. (2012). GADD45 proteins: central players in tumorigenesis. Curr. Mol. Med. *12*, 634–651.

Taranova, O.V., Magness, S.T., Fagan, B.M., Wu, Y., Surzenko, N., Hutton, S.R., and Pevny, L.H. (2006). SOX2 is a dose-dependent regulator of retinal neural progenitor competence. Genes Dev *20*, 1187–1202.

Tirosh, I., Izar, B., Prakadan, S.M., Wadsworth, M.H., Treacy, D., Trombetta, J.J., Rotem, A., Rodman, C., Lian, C., Murphy, G., et al. (2016). Dissecting the multicellular ecosystem of metastatic melanoma by single-cell RNA-seq. Science *352*, 189–196.

Tomic, G., Morrissey, E., Kozar, S., Ben-Moshe, S., Hoyle, A., Azzarelli, R., Kemp, R., Chilamakuri, C.S.R., Itzkovitz, S., Philpott, A., et al. (2018). Phospho-regulation of ATOH1 Is Required for Plasticity of Secretory Progenitors and Tissue Regeneration. Cell Stem Cell *23*, 436-443.e7.

Tran, N.M., Shekhar, K., Whitney, I.E., Jacobi, A., Benhar, I., Hong, G., Yan, W., Adiconis, X., Arnold, M.E., Lee, J.M., et al. (2019). Single-Cell Profiles of Retinal Ganglion Cells Differing in Resilience to Injury Reveal Neuroprotective Genes. Neuron *104*, 1039-1055.e12.

Trimarchi, J.M., Stadler, M.B., Roska, B., Billings, N., Sun, B., Bartch, B., and Cepko, C.L. (2007). Molecular heterogeneity of developing retinal ganglion and amacrine cells revealed through single cell gene expression profiling. J Comp Neurol *502*, 1047–1065.

Trimarchi, J.M., Stadler, M.B., and Cepko, C.L. (2008). Individual retinal progenitor cells display extensive heterogeneity of gene expression. PLoS One *3*, e1588.

Usui, A., Mochizuki, Y., Iida, A., Miyauchi, E., Satoh, S., Sock, E., Nakauchi, H., Aburatani, H., Murakami, A., Wegner, M., et al. (2013). The early retinal progenitor-expressed gene Sox11 regulates the timing of the differentiation of retinal cells. Development *140*, 740–750.

Wall, D.S., Mears, A.J., McNeill, B., Mazerolle, C., Thurig, S., Wang, Y., Kageyama, R., and Wallace, V.A. (2009). Progenitor cell proliferation in the retina is dependent on Notch-independent Sonic hedgehog/Hes1 activity. J Cell Biol *184*, 101–112.

Wang, F., Flanagan, J., Su, N., Wang, L.C., Bui, S., Nielson, A., Wu, X., Vo, H.T., Ma, X.J., and Luo, Y. (2012). RNAscope: a novel in situ RNA analysis platform for formalin-fixed, paraffin-embedded tissues. J Mol Diagn *14*, 22–29.

Wang, S.W., Gan, L., Martin, S.E., and Klein, W.H. (2000). Abnormal polarization and axon outgrowth in retinal ganglion cells lacking the POU-domain transcription factor Brn-3b. Mol Cell Neurosci *16*, 141–156.

Wang, S.W., Kim, B.S., Ding, K., Wang, H., Sun, D., Johnson, R.L., Klein, W.H., and Gan, L. (2001). Requirement for math5 in the development of retinal ganglion cells. Genes Dev *15*, 24–29.

Wang, Y., Dakubo, G.D., Thurig, S., Mazerolle, C.J., and Wallace, V.A. (2005). Retinal ganglion cell-derived sonic hedgehog locally controls proliferation and the timing of RGC development in the embryonic mouse retina. Development *132*, 5103–5113.

Wong, L.L., and Rapaport, D.H. (2009). Defining retinal progenitor cell competence in Xenopus laevis by clonal analysis. Development *136*, 1707–1715.

Wu, F., Sapkota, D., Li, R., and Mu, X. (2012). Onecut 1 and Onecut 2 are potential regulators of mouse retinal development. J Comp Neurol *520*, 952–969.

Wu, F., Kaczynski, T.J., Sethuramanujam, S., Li, R., Jain, V., Slaughter, M., and Mu, X. (2015). Two transcription factors, Pou4f2 and Isl1, are sufficient to specify the retinal ganglion cell fate. Proc Natl Acad Sci U A *112*, E1559-68.

Xiang, M. (2013). Intrinsic control of mammalian retinogenesis. Cell Mol Life Sci *70*, 2519–2532.

Xiang, M., Zhou, L., Macke, J.P., Yoshioka, T., Hendry, S.H., Eddy, R.L., Shows, T.B., and Nathans, J. (1995). The Brn-3 family of POU-domain factors: primary structure, binding specificity, and expression in subsets of retinal ganglion cells and somatosensory neurons. J Neurosci *15*, 4762–4785.

Yang, Z., Ding, K., Pan, L., Deng, M., and Gan, L. (2003). Math5 determines the competence state of retinal ganglion cell progenitors. Dev Biol *264*, 240–254.

Yaron, O., Farhy, C., Marquardt, T., Applebury, M., and Ashery-Padan, R. (2006). Notch1 functions to suppress cone-photoreceptor fate specification in the developing mouse retina. Development *133*, 1367–1378.

Young, R.W. (1985). Cell differentiation in the retina of the mouse. Anat Rec *212*, 199–205.

Yuniati, L., Scheijen, B., van der Meer, L.T., and van Leeuwen, F.N. (2019). Tumor suppressors BTG1 and BTG2: Beyond growth control. J. Cell. Physiol. *234*, 5379–5389.

Zhang, Q., Zagozewski, J., Cheng, S., Dixit, R., Zhang, S., de Melo, J., Mu, X., Klein, W.H., Brown, N.L., Wigle, J.T., et al. (2017). Regulation of Brn3b by DLX1 and DLX2 is required for retinal ganglion cell differentiation in the vertebrate retina. Dev. Camb. Engl. *144*, 1698–1711.

Zhao, S., Chen, Q., Hung, F.-C., and Overbeek, P.A. (2002). BMP signaling is required for development of the ciliary body. Development *129*, 4435–4442.

Zheng, G.X.Y., Terry, J.M., Belgrader, P., Ryvkin, P., Bent, Z.W., Wilson, R., Ziraldo, S.B., Wheeler, T.D., McDermott, G.P., Zhu, J., et al. (2017). Massively parallel digital transcriptional profiling of single cells. Nat. Commun. *8*, 1–12.

Zhou, H., Yoshioka, T., and Nathans, J. (1996). Retina-derived POU-domain factor-1: a complex POU-domain gene implicated in the development of retinal ganglion and amacrine cells. J Neurosci *16*, 2261–2274.

Figure legends:

Figure 1. Conventional RNA-seq identifies differentially expressed genes (DEGs) in E14.5 *Atoh7*-null, *Pou4f2*-null, and *Isl1*-null retinas. A. Clustering of all DEGs across all four genotypes based on Z score indicates the *Atoh7*-null retina is least similar, whereas the Isl1-null retina is most similar to the wild-type retina. The genes was divided into five groups (1-5) based on how they are affected in the three mutants. B. A Venn-diagram showing the overlaps of downregulated genes in all three mutant retinas. C. A Venn-diagram showing the overlaps of upregulated genes in the three mutant retinas.

Figure 2. The Shh pathway is regulated by the RGC gene regulatory cascade at multiple levels. A. Multiple component genes of the Shh pathway are downregulated in the three mutant retinas. Error bars are standard deviation. P values between all mutants and wild-type were all smaller than 0.001. B. A diagram showing how Atoh7-Pou4f2/Isl1 gene regulatory cascade regulates the Shh pathway in the developing retina in a complex manner, with multiple feedback loops.

Figure 3. Single cell RNA-seq (scRNA-seq) analysis of E13.5 wild-type and *Atoh7*-null retinas. A. B. As indicated, UMAP clustering leads to the same 11 overlapping clusters (C0-C10) with both wild-type (A) and *Atoh7*-null (B) retinal cells. C. Expression of known markers genes as represented by a dot plot enables identity assignment of individual wild-type clusters (see text for details). As indicated, the sizes of the dots indicate the percentage of cells expressing the gene in individual clusters and the color intensities denote average expression levels. D. E. Cell cycle analysis determines the cell cycle status (G1, S, and G2/M) of individual cells in the clusters. Note that largely the same cell cycle distribution is observed in the wild-type (D) and *Atoh7*-null (E) retinas, and that the cell cycle statuses correlate with UMPA clustering.

Figure 4. Cluster-specific gene expression reveals the relationships among the wild-types clusters. A. A heatmap showing the top ten enriched genes in each cluster. Each horizontal line represents one gene and each vertical line represents one cell. Data from equal numbers (100) of cells from each cluster are shown. The heatmap clearly demonstrates the continuity and directionality between these clusters. B. A Venn diagram showing the overlaps of enriched genes between naïve RPCs (nRPCs, C0-C2), transitional RPCs (tRPCs, C3 and C4), and RGCs (C5 and C6). tRPCs have substantial overlaps with both nRPCs and RGCs, but nRPC and RGCs have very few overlapped genes, indicating the unidirectional relationship of these clusters. C. D. Developmental trajectories predicted by the SCANPY tool based on diffusion pseudotime (DPT). Three trajectories representing the emergence of photoreceptor (PH), horizontal and amacrine cells (H&A), and RGCs from RPCs are clearly identified for both the wild-type (C) and Atoh7-null (D) cells. Progression is color-coded and the direction of each lineage is clearly discernible, although the RGC lineage of the Atoh7-null cells does not advance as far as the wild-type cells.

Figure 5. Spatial expression of *Sox4* and *Sox11*. A. Feature plot heatmaps indicate that both genes are expressed in all clusters but at much higher levels in differentiating cells, and that their expression levels are comparable in the *Atoh7*-null (MT) cells. B. Violin plots indicate that both genes are expressed in comparable levels in corresponding wild-type (WT, red) and *Atoh7*-null (MT, blue) clusters. The heights of the plots represent expression levels and the widths represent relative proportions of cells expressing the gene at that level. D. E. In situ hybridization with RNAscope probes confirms that *Sox4* and *Sox11* are expressed in both RPCs and RGCs. Note that both genes are highly expressed in a subset of RPCs in the outside part of the retina, which presumably are the transitional RPCs.

Figure 6. Gene expression signature of transitional RPCs (C3, C4). A. Genes regulating distinct lineages are expressed in a shared transitional state, namely transitional RPCs, as demonstrated by a dot plot. Often these genes continue to be expressed in the specific cell lineage they regulate, e.g. *Atoh7* and *Sox11* in RGCs (C5), and *Otx2* in photoreceptors (C8, C9). B. Additional genes, including many encoding components of the Notch pathway, are enriched in the transitional RPCs (C3, C4). C. Feature heatmap showing the expression of *Atoh7*, *Neurod1,* and *Otx2* in the wild-type clusters. The dotted line demarcates transitional RPCs (C3 and C4). Consistent with the dot plot, all three genes are expressed in transitional RPCs, but *Atoh7* is expressed in more transitional RPCs than *Neurod1* and *Otx2*. Whereas *Atoh7* trails into all three lineages, *Neurod1* and *Otx2* only continue to be expressed in photoreceptors. D. In situ hybridization with RNAscope probes confirms that *Gadd45a* and *Btg2* are expressed in a subset of RPCs with a pattern similar to *Atoh7* in all three developmental stages (E12.5, E14.5, E16.5) examined.

Figure 7. Gene expression underlying the RGC lineage in the *Atoh7*-null retina. A. Overlaps of down- and upregulated DEGs (DN and UP respectively) in *Atoh7*-null RGCs and RGC-enriched genes (EN) as presented by a Venn diagram. B. Euclidean distance clustering demonstrating seven different modes of changes in gene expression in *Atoh7*-null retinal RGCs (C5 andC6, see main text for details). For comparison, expression in C3 and C4 are also presented. C. Example genes with different modes of expression as demonstrated by violin plots, showing their expression across all clusters of wild-type (WT, red) and *Atoh7*-null (MT, blue) cells. The heights of the plots represent expression levels and the widths represent relative proportions of cells expressing the gene at that level. *Pou4f2* is from group 1a in B, *Syt4*, *Pou6f2*, *Gap43*, and *Elavl4* are from group 1b, *Nhlh2* is from group 2, *Kctd8* is from group 3a, and *Neurod1* is from group 3b.

Figure 8. A model explaining shifts of cell states along the RGC trajectory in the wild-type and *Atoh7*-null retina. The RGC trajectory follows several distinct cell states, including naïve RPCs, transitional RPCs, nascent RGCs, and differentiated RGCs. The direction of the trajectory is indicated by the arrow and the progression of the trajectory is indicated by a color gradient. Each state is determined by a group of genes and example genes are given in colored circles. The transition from one state to the next is dictated by

downregulation of genes representing that state and upregulation of genes for the next state as indicated by the sizes of the colored circles. In the transitional RPCs, Atoh7, likely in combination with the SoxC factors, competes with other regulators to drive them to the RGC fate. In the *Atoh7*-null retina, the establishment of the transitional RPC state is not affected, and nascent RGCs still form through expression of some, but not all, RGC genes (represented by a smaller circle with broken lines). The mutant nascent RGCs fail to reach the full RGC state and eventually die by apoptosis (indicated by a striped background).

Supplemental figure legends

Supplemental Figure 1. Feature plots demonstrating the cluster-specific expression of marker genes in both wild-type and *Atoh7*-null (knockout) retinas. These markers were used to assign identities to the clusters, including *Ccnd1* and *Fgf15* for naïve RPCs, *Atoh7* and *Otx2* for transitional RPCs, *Pou4f2* and P*ou6f2* for RGCs, *Ptf1a* and *Tfap2b* for amacrine and horizontal precursors, *Neurod4* and *Crx* for photoreceptors, and *Otx1* and *Gja1* for ciliary margin cells. Note that that expression of *Atoh7* and the two RGC marker genes *Pou4f2* and *Pou6f2* are diminished in the knockout cells.

Supplemental Figure 2. Feature plots based on scRNA-seq showing the expression patterns of five naïve RPC enriched genes and ten RGC-enriched genes. Comparing with in situ hybridization (see Suppl. Figure 3), scRNA-seq provides more details of cell type-specific expression. For example, *Fbxo5* is expressed only in subsets of naïve RPCs and transitional RPCs, which are likely in the late S/early G2/M phase of the cell cycle (compare with Figure 3D).

Supplemental Figure 3. In situ hybridization confirms the spatial expression patterns of five naïve RPC enriched genes and ten RGC-enriched genes. The in situ hybridization data were obtained from the Eurexpress database and match well with the enrichment results from our scRNA-seq analysis (See Suppl. Figure 2 and Suppl. Table 5).

Supplemental Figure 4. Comparison of wild-type and *Atoh7*-null clusters. A. Proportions of cells in each wild-type (WT, blue) and *Atoh7*-null (MT, red) clusters. Nascent RGCs (C5) and differentiated RGCs (C5) are highlighted by a red box. Note there is no major change in the proportion of cells in C5, but a marked reduction in C6. B. Scatter plots comparing gene expression in corresponding pairs of wild-type (WT) and *Atoh7*-null (MT) clusters. The correlation coefficients (R^2) are shown for each pair. The C5 and C6 pairs have the lowest R^2 values, indicating the most changes in gene expression.

Figure 1

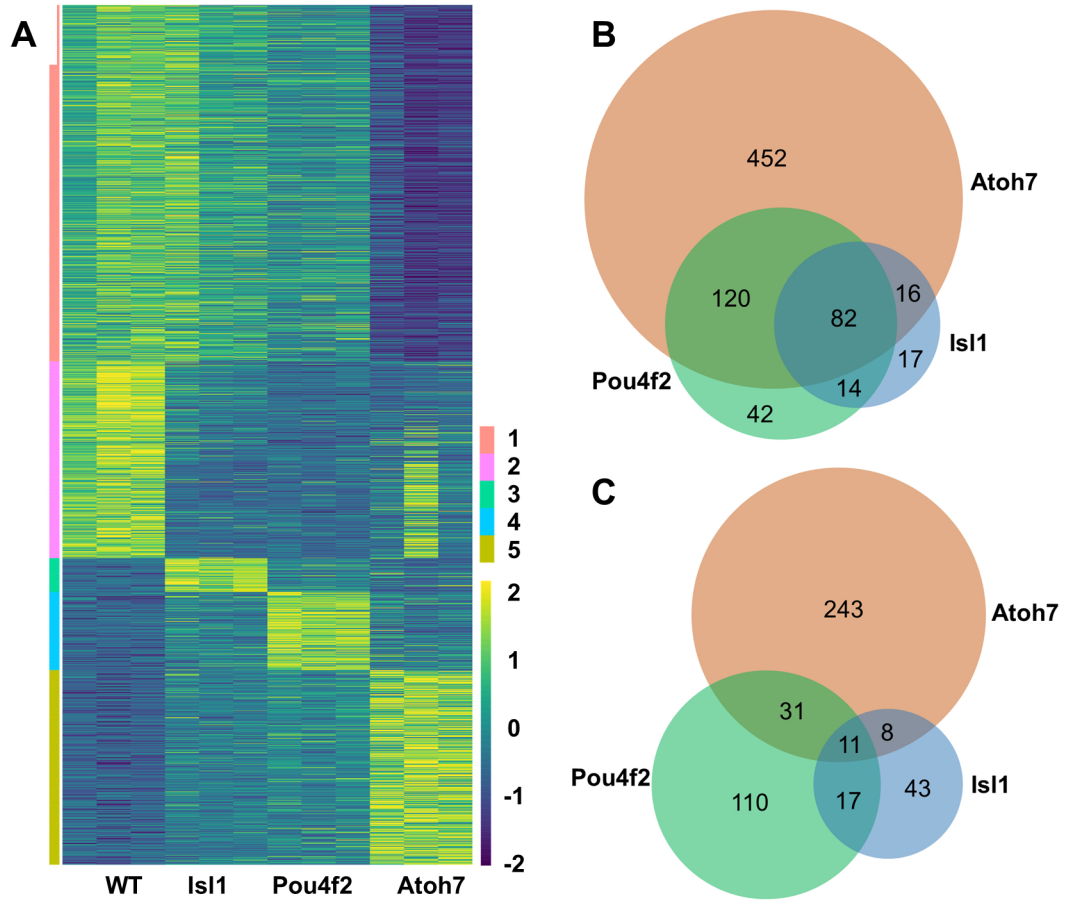
A
1
2
3
4
5
2
1
0
-1
-2
WT
Isl1
Pou4f2
Atoh7
B
452
Atoh7
120
82
16
Isl1
17
Pou4f2
14
42
C
243
Atoh7
31
11
8
Pou4f2
110
17
43
Isl1

Figure 2

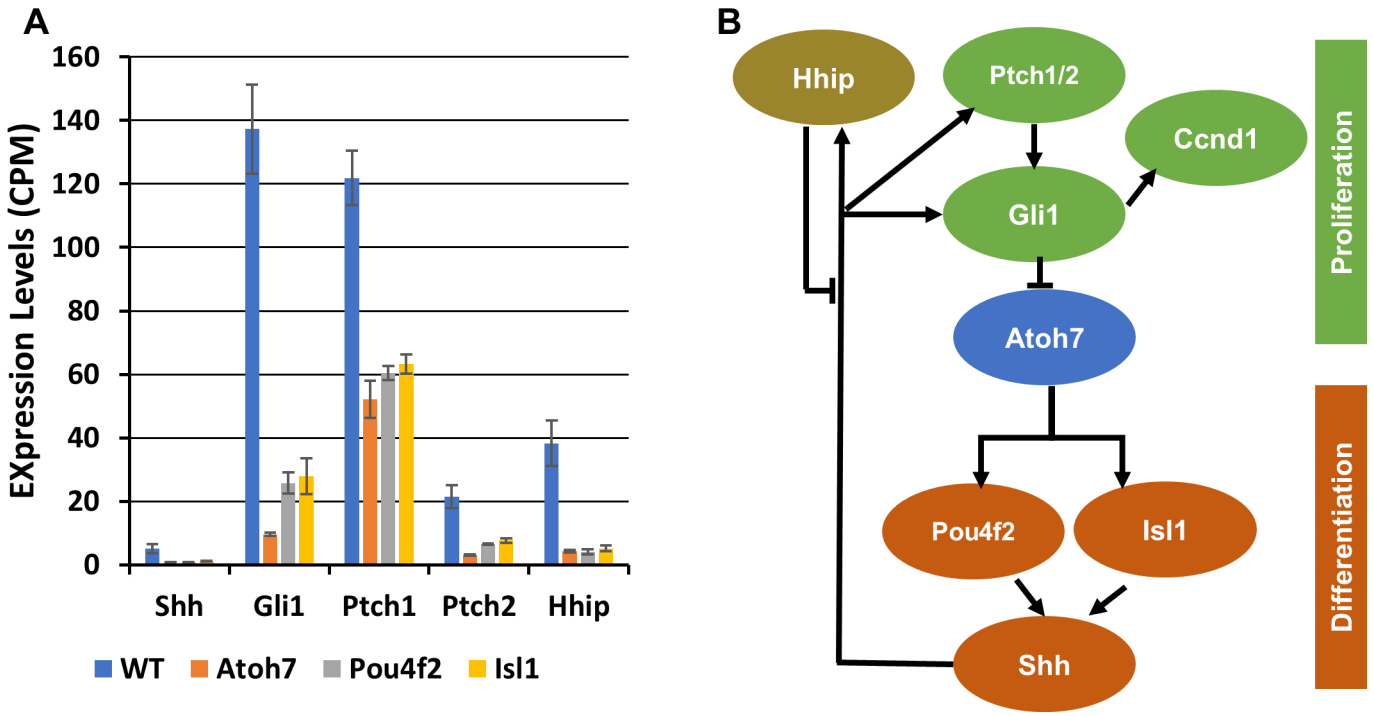
A
EXpression Levels (CPM)
160
140
120
100
80
60
40
20
0
Shh
Gli1
Ptch1
Ptch2
Hhip
WT
Atoh7
Pou4f2
Isl1
B
Hhip
Ptch1/2
Ccnd1
Gli1
Atoh7
Pou4f2
Isl1
Shh
Proliferation
Differentiation

Figure 3

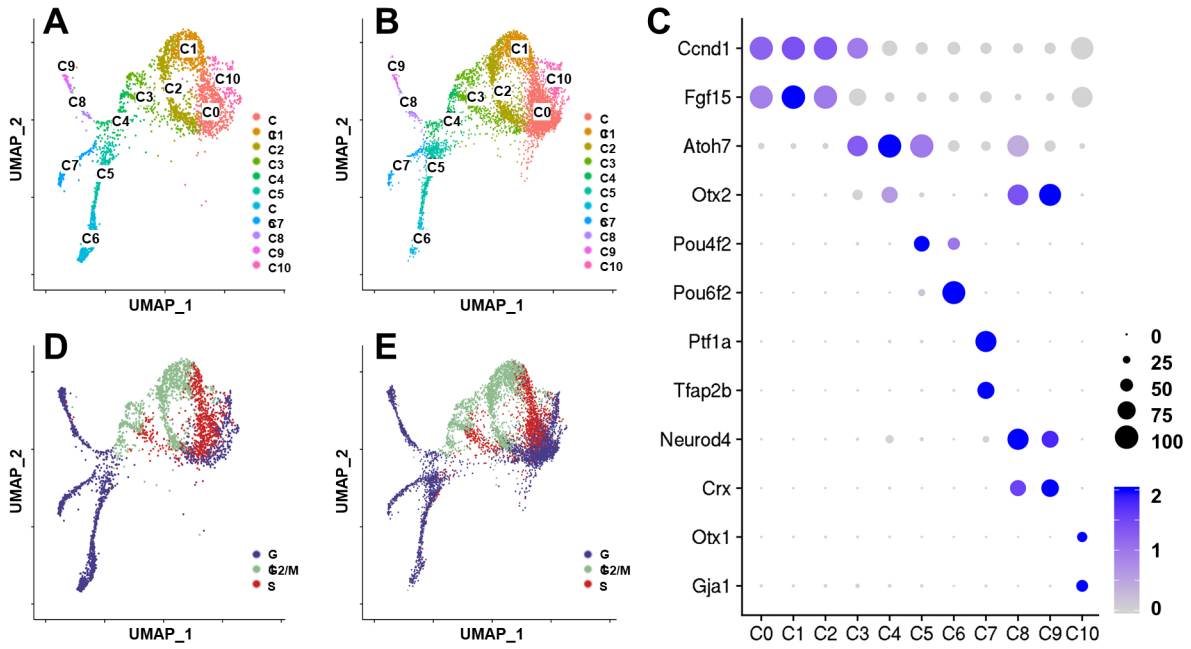
A
B
C
D
E
UMAP_1
UMAP_2
C0
C1
C2
C3
C4
C5
C6
C7
C8
C9
C10
G2/M
S
Ccnd1
Fgf15
Atoh7
Otx2
Pou4f2
Pou6f2
Ptf1a
Tfap2b
Neurod4
Crx
Otx1
Gja1
0
25
50
75
100
2
1
0

Figure 4

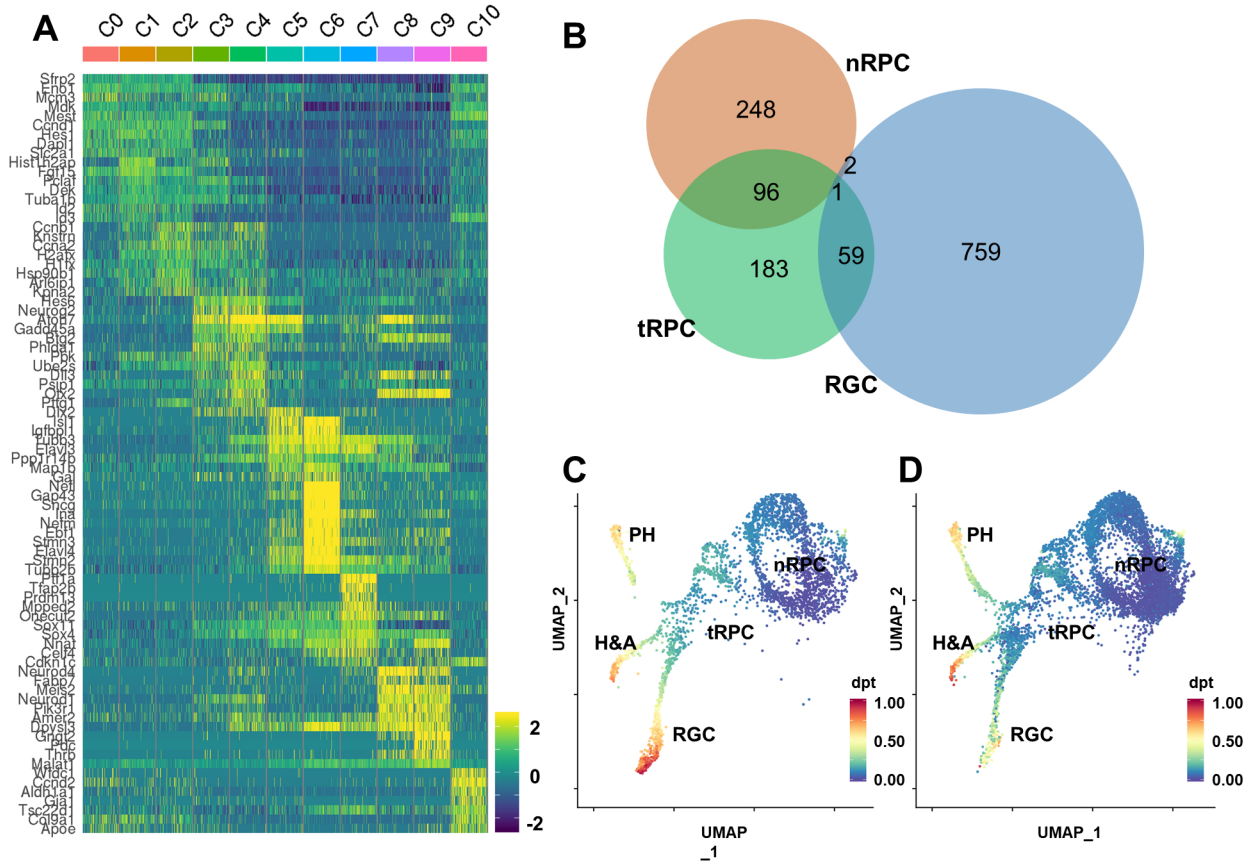
A
C0
C1
C2
C3
C4
C5
C6
C7
C8
C9
C10
2
0
-2
B
nRPC
248
2
96
1
183
59
759
tRPC
RGC
C
PH
nRPC
H&A
tRPC
RGC
dpt
1.00
0.50
0.00
UMAP_2
UMAP_1
D
PH
nRPC
H&A
tRPC
RGC
dpt
1.00
0.50
0.00
UMAP_2
UMAP_1

Figure 5

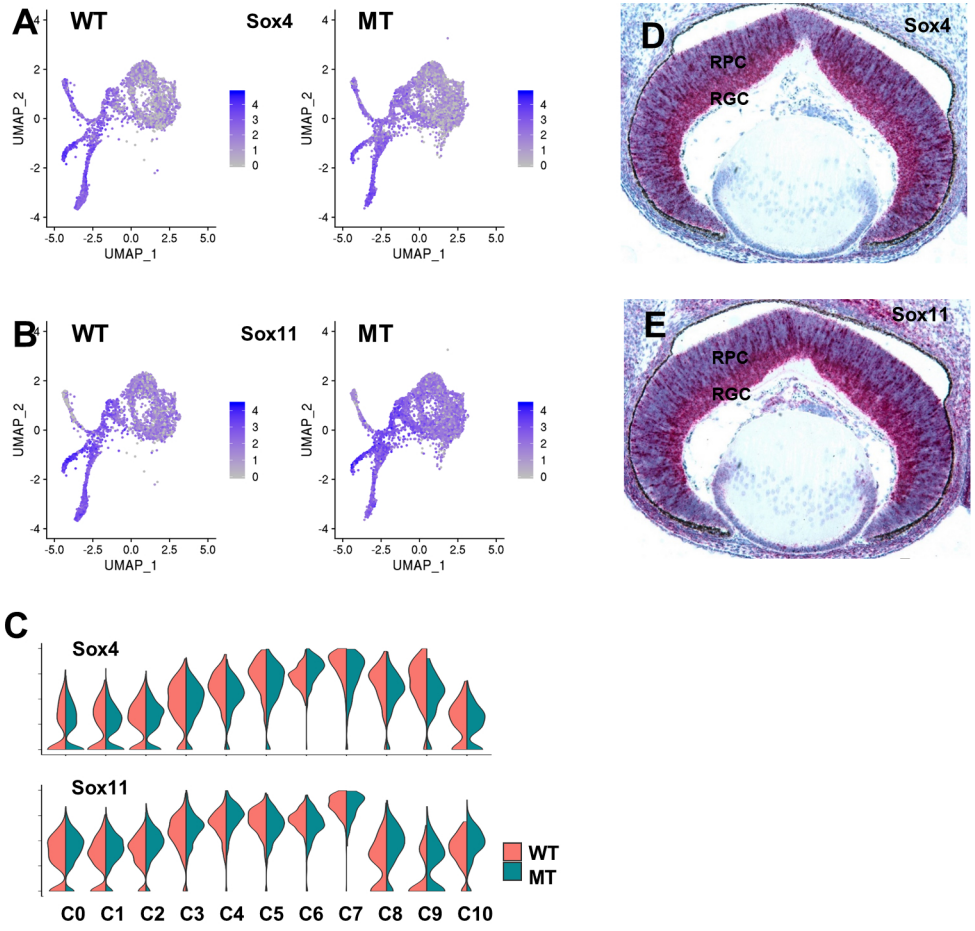
A
WT
Sox4
MT
UMAP_2
UMAP_1
B
WT
Sox11
MT
C
Sox4
Sox11
WT
MT
C0 C1 C2 C3 C4 C5 C6 C7 C8 C9 C10
D
Sox4
RPC
RGC
E
Sox11
RPC
RGC

Figure 6

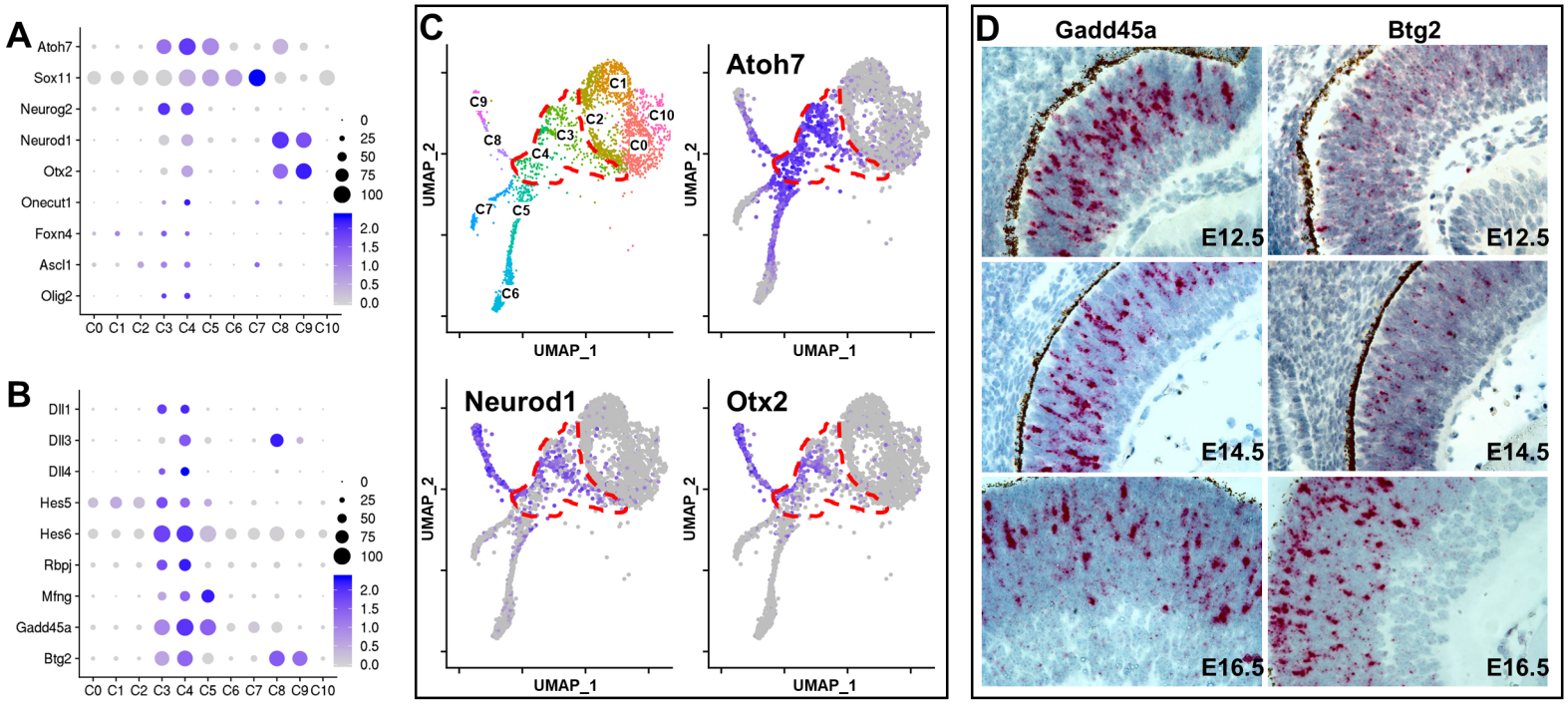
A
Atoh7
Sox11
Neurog2
Neurod1
Otx2
Onecut1
Foxn4
Ascl1
Olig2
C0 C1 C2 C3 C4 C5 C6 C7 C8 C9 C10
0
25
50
75
100
2.0
1.5
1.0
0.5
0.0
B
Dll1
Dll3
Dll4
Hes5
Hes6
Rbpj
Mfng
Gadd45a
Btg2
C0 C1 C2 C3 C4 C5 C6 C7 C8 C9 C10
C
C9
C1
C2
C10
C8
C3
C4
C0
C7
C5
C6
UMAP_2
UMAP_1
Atoh7
Neurod1
Otx2
D
Gadd45a
Btg2
E12.5
E14.5
E16.5

Figure 7

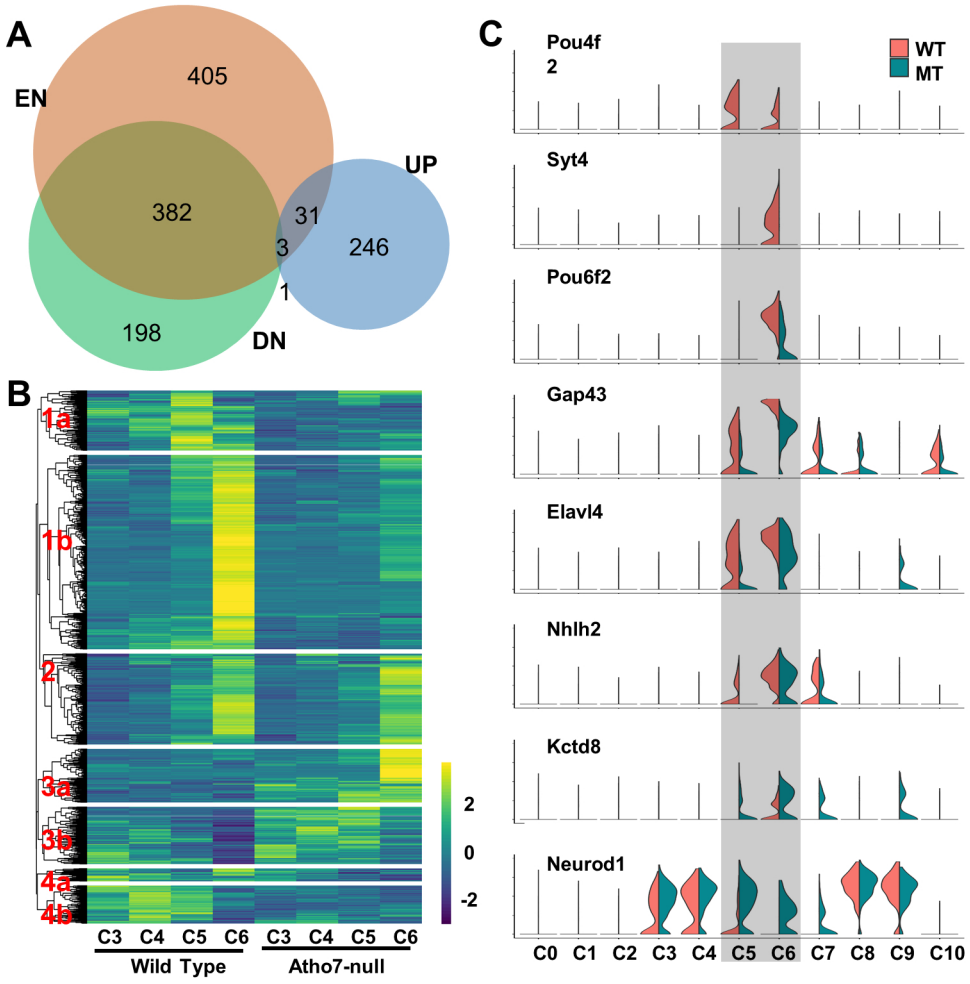
A
EN
405
382
31
3
246
1
198
DN
UP
B
1a
1b
2
3a
3b
4a
4b
C3 C4 C5 C6 C3 C4 C5 C6
Wild Type
Atho7-null
2
0
-2
C
Pou4f
2
WT
MT
Syt4
Pou6f2
Gap43
Elavl4
Nhlh2
Kctd8
Neurod1
C0 C1 C2 C3 C4 C5 C6 C7 C8 C9 C10

Figure 8

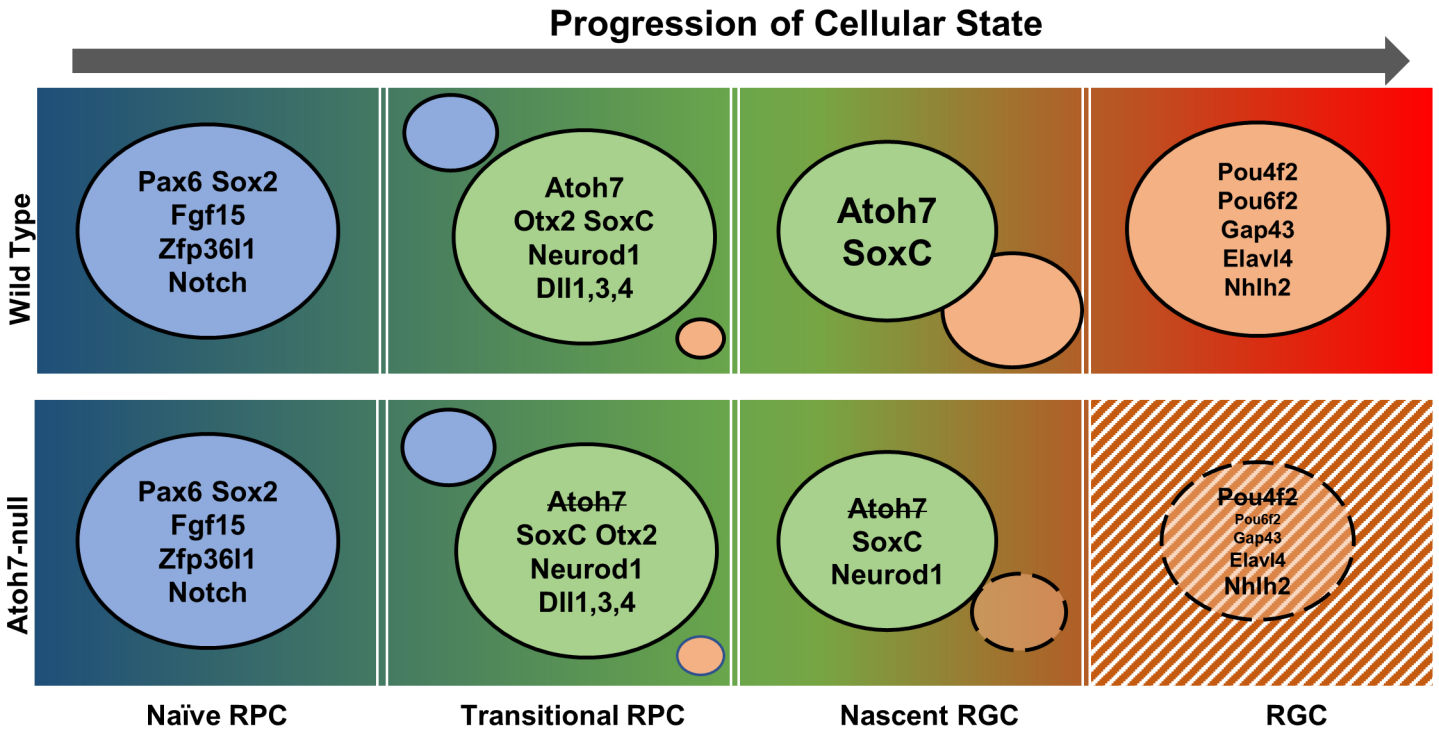
Progression of Cellular State
Wild Type
Pax6 Sox2
Fgf15
Zfp36l1
Notch
Atoh7
Otx2 SoxC
Neurod1
Dll1,3,4
Atoh7
SoxC
Pou4f2
Pou6f2
Gap43
Elavl4
Nhlh2
Atoh7-null
Pax6 Sox2
Fgf15
Zfp36l1
Notch
~~Atoh7~~
SoxC Otx2
Neurod1
Dll1,3,4
~~Atoh7~~
SoxC
Neurod1
~~Pou4f2~~
Pou6f2
Gap43
Elavl4
Nhlh2
Naïve RPC
Transitional RPC
Nascent RGC
RGC

Suppl. Figure 1

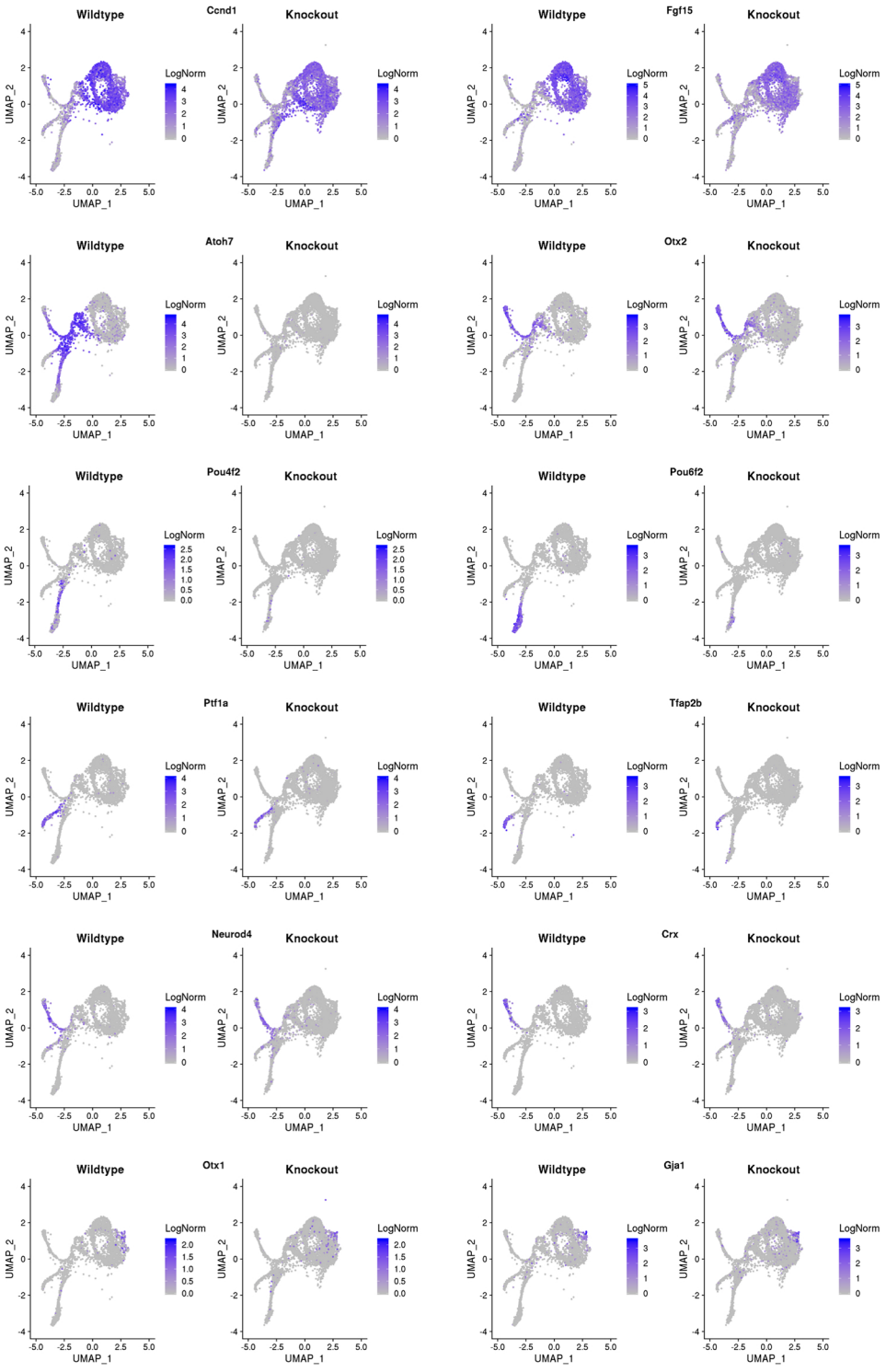

Suppl. Figure 2

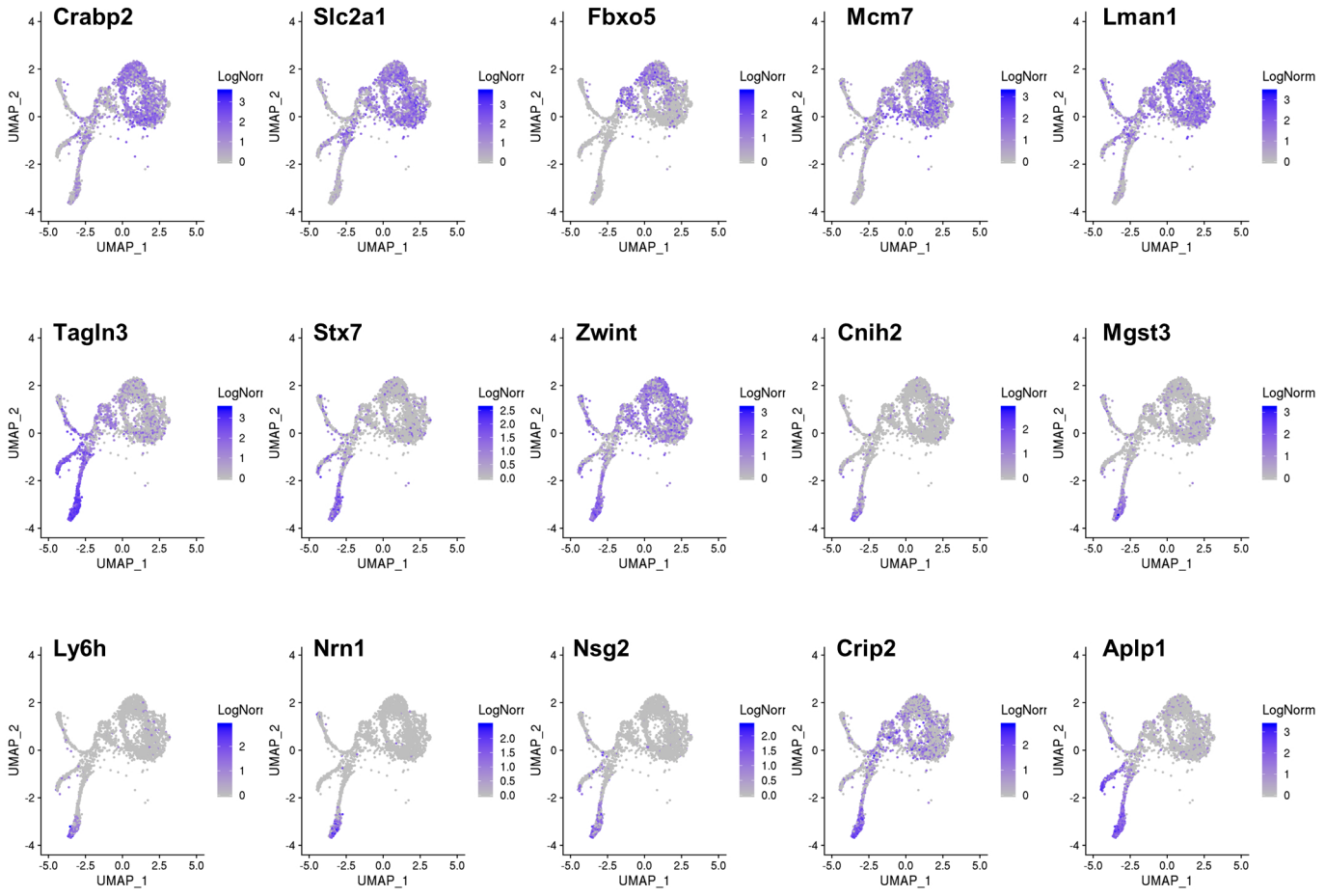

Suppl. Figure 3

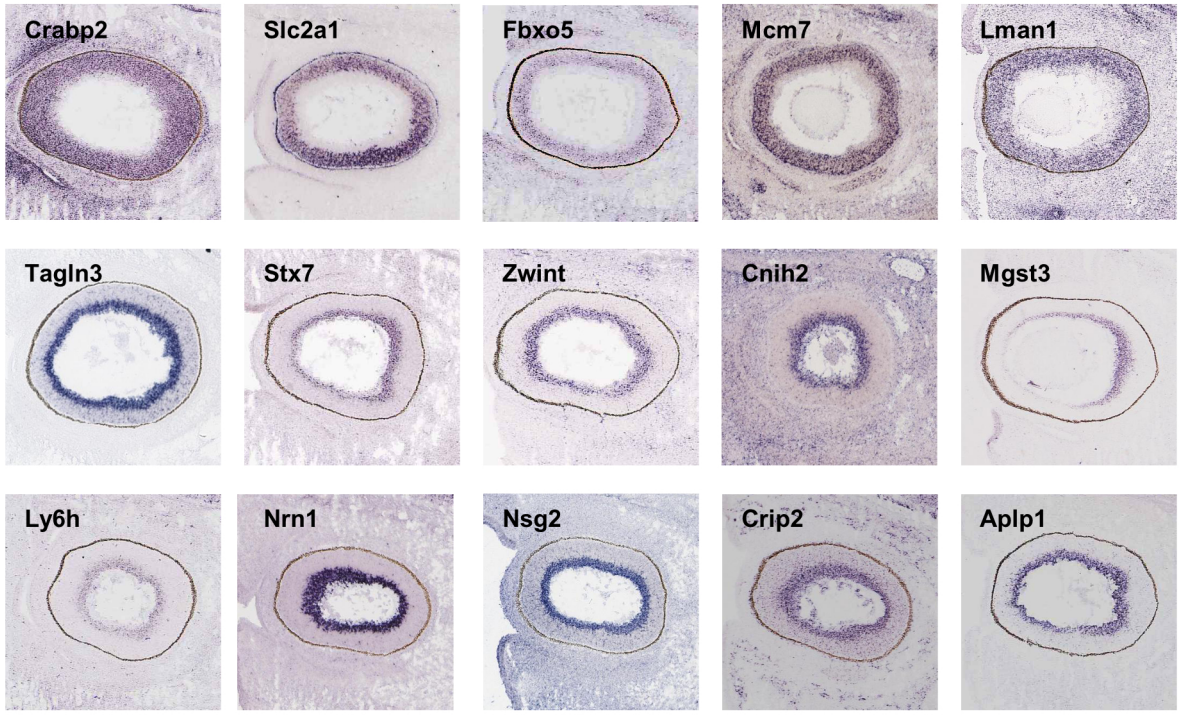

Suppl. Figure 4

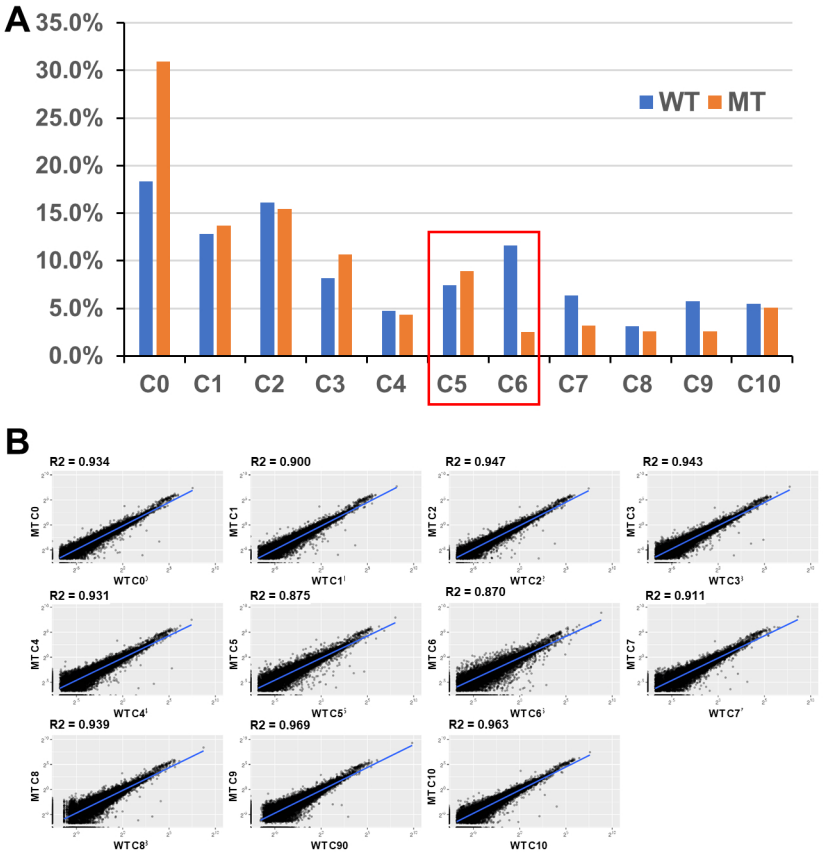

Table 1. Enriched GO terms for individual cell states/types

Term	Count	%	Fold Enrichment	P Value
Naïve RPCs (C0-C3)				
cell cycle	64	18.66	5.84	2.63E-30
cell division	51	14.87	7.63	2.13E-29
mitotic nuclear division	42	12.24	8.49	6.07E-26
nucleosome assembly	22	6.41	11.84	1.20E-16
chromosome segregation	16	4.66	10.06	4.83E-11
Transitional RPCs (C3, C4)				
RNA splicing	35	10.42	8.42	1.85E-21
cell cycle	51	15.18	4.81	2.52E-20
mRNA processing	37	11.01	6.66	3.06E-19
cell division	34	10.12	5.27	1.29E-14
mRNA splicing, via spliceosome	19	5.65	9.83	7.01E-13
RGCs (C5, C6)				
nervous system development	63	7.67	4.07	3.24E-21
axon guidance	31	3.78	5.07	3.39E-13
axonogenesis	25	3.05	5.69	7.00E-12
neuron projection development	24	2.92	4.21	1.07E-08
substantia nigra development	13	1.58	8.34	2.08E-08
Photoreceptors (C8, C9)				
nervous system development	30	8.17	4.35	7.13E-11
axon guidance	16	4.36	5.87	9.73E-08
cell differentiation	34	9.26	2.38	6.70E-06
neuron migration	12	3.27	5.29	1.71E-05
multicellular organism development	38	10.35	2.02	6.55E-05
Amacrine and Horizontal Cells (C7)				
visual perception	13	3.80	5.99	1.82E-06
photoreceptor cell maintenance	7	2.05	10.73	4.23E-05
synaptic vesicle exocytosis	5	1.46	16.13	2.19E-04
negative regulation of transcription from RNA polymerase II promoter	26	7.60	2.19	3.79E-04
positive regulation of transcription from RNA polymerase II promoter	32	9.36	1.97	4.08E-04